JOURNAL OF GEOPHYSICAL RESEARCH, VOL. 107, NO. B10, 2253, doi:10.1029/2001JB000672, 2002

Paleomagnetism of Paleozoic and Mesozoic sediments from the southern margin of Mongol-Okhotsk ocean, far eastern Russia

Vadim A. Kravchinsky[1]
Physics Department, University of Alberta, Edmonton, Canada

Andrey A. Sorokin
Division of the Regional Geology and Hydrogeology, Far East Branch of Russian Academy of Science, Blagoveshchensk, Russia

Vincent Courtillot
Laboratoire de Paléomagnétisme, Institut de Physique du Globe de Paris, Paris, France

Received 15 June 2001; revised 1 March 2002; accepted 6 March 2002; published 24 October 2002.

[1] This paper presents new data from paleomagnetic investigations of Middle Paleozoic (Early-Middle-Late Devonian, Early Carboniferous) and Middle Jurassic geological units from the Amuria block south of the Mongol-Okhotsk suture zone. With fold tests for all localities, and two polarities for the Devonian, our new results constrain the evolution of the Mongol-Okhotsk ocean from the Devonian to the Middle Jurassic. The corresponding paleopoles lie at 21.6°N, 6.3°E (dp/dm = 5.3°/10.6°) for Early Devonian, 26.3°N, 345.3°E (dp/dm = 6.4°/12.8°) for Early-Middle Devonian, 24.6°N, 12.9°E (dp/dm = 8.7°/16.9°) for Middle-Late Devonian, 40.5°N, 352.4°E (dp/dm = 9°/16.7°) for Late Devonian, 39.8°N, 31.6°E (dp/dm = 10°/15.5°) for Early Carboniferous, and 46°N, 37.9°E (dp/dm = 9.4°/13.4°) for Middle Jurassic. The poles confirm that the large Paleozoic Mongol-Okhotsk ocean closed during the Jurassic, ending up in the late Jurassic or early Cretaceous at the eastern end of the suture zone, as originally proposed on geological grounds. The new paleomagnetic results exhibit large tectonic rotations about local vertical axes, which we interpret as probably arising from both the collision process and left-lateral shear movement along the suture zone, related to incipient extrusion of Amuria due to indentation of India into Asia. *INDEX TERMS:* 1525 Geomagnetism and Paleomagnetism: Paleomagnetism applied to tectonics (regional, global); 1744 History of Geophysics: Tectonophysics; 8149 Tectonophysics: Planetary tectonics (5475); *KEYWORDS:* Amuria, Mongol-Okhotsk ocean, paleomagnetism, plate tectonic, Siberia, suture

Citation: Kravchinsky, V. A., A. A. Sorokin, and V. Courtillot, Paleomagnetism of Paleozoic and Mesozoic sediments from the southern margin of Mongol-Okhotsk ocean, far eastern Russia, *J. Geophys. Res.*, *107*(B10), 2253, doi:10.1029/2001JB000672, 2002.

1. Introduction

[2] The eastern part of Eurasia is a complex collage consisting of both large and small continental blocks separated by Paleozoic and Mesozoic fold belts formed in the locations of former paleo-ocean basins. One of the largest structures is the Mongol-Okhotsk fold belt in the far eastern part of Russia. This belt is a complex system, comprising fragments of E-W trending Paleozoic and Early Mesozoic structures, between the southern margin of the Siberian craton to the north and the Amurian composite microcontinent to the south (Figure 1). According to recent geodynamic reconstructions, the belt is regarded as consisting of relics of a vast ocean, now preserved as a complex set of terranes, squeezed between the above mentioned continental masses [*Zonenshain et al.*, 1990; *Natal'in and Borukaev*, 1991; *Parfenov et al.*, 1999].

[3] At present, the issue concerning the width of the Mongol-Okhotsk paleo-ocean as well as the timing and kinematics of its closure remain unresolved. According to commonly accepted models, the vast Mongol-Okhotsk ocean existed from the Riphean up to the Early [*Sengor and Natal'in*, 1996] or Late [*Zonenshain et al.*, 1990] Jurassic, and closed in a scissors manner [*Zonenshain et al.*, 1990; *Zhao et al*, 1990], or may have formed as the result of sliding of the Amurian microcontinent along the southern margin of the Siberian craton [*Parfenov et al.*, 1999].

[1]Also at Institute of Geochemistry, Siberian Branch of Russian Academy of Science, Irkutsk, Russia.

Copyright 2002 by the American Geophysical Union.
0148-0227/02/2001JB000672$09.00

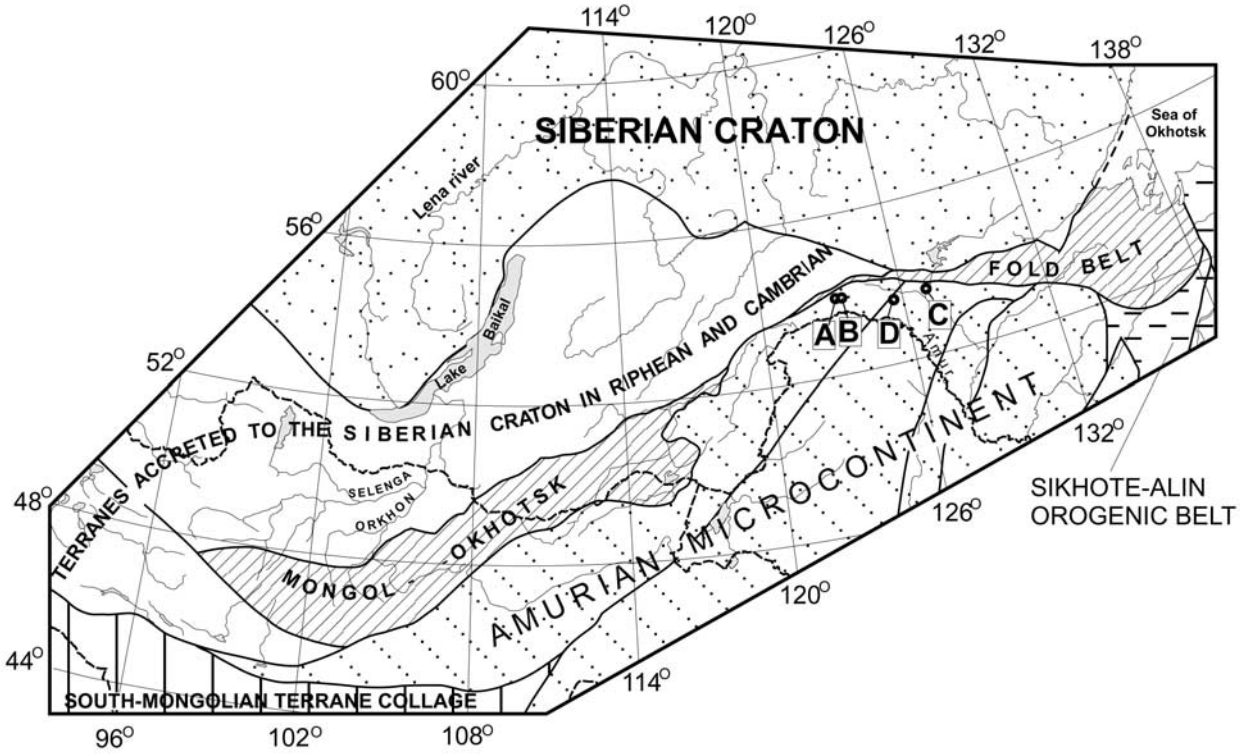

Figure 1. Location of the sampling sites relatively to main tectonic structures of the region. (Tectonic sketch map is modified after *Parfenov et al.* [1999].) Sampling sites are shown by dots with letters: A, Oldoy; B, Imachi; C, Zeya; D, Taldan. A–C, this study area; D, area studied by *Halim et al.* [1998a]. Geological sketch maps of sites A–C are shown in Figures 2 and 3.

[4] Paleomagnetic data published in the geological literature which should define the paleoposition of the Siberian and north China cratons, show significant discrepancies in paleolatitudes up to Early Cretaceous time [*Zhao et al.*, 1996; *Enkin et al.*, 1992; *Gilder and Courtillot*, 1997; *Kravchinsky*, 1995, 2002a; *Smethurst et al.*, 1998]. Also, there are not enough reliable paleomagnetic data from many of the blocks, which comprise the Amurian microcontinent. We have studied Paleozoic and Mesozoic sedimentary deposits located south of the Mongol-Okhotsk suture (Upper Amur region), which represent the largest part of the Amurian microcontinent. This allows us to estimate the width of the Mongol-Okhotsk ocean as a function of time and to constrain kinematic models of its closure.

2. Brief Geological Review

[5] Paleo-oceanic structures within the Mongol-Okhotsk fold belt comprise ophiolite fragments, metabasaltic chert, and also turbidites and terrigenous-carbonaceous deposits [*Sorokin et al.*, 1996]. Paleontological observations allow one to identify Devonian and Carboniferous sediments, and within the eastern segment, Lower and Upper Permian, Triassic and Lower Jurassic ones [*Kozlovsky*, 1988; *Parfenov et al.*, 1999]. Along the southern rim of the Mongol-Okhotsk fold belt, a system of paleobasins filled with Paleozoic and Mesozoic sediments is found. These are interpreted as passive continental margins [*Zonenshain et al.*, 1990; *Parfenov et al.*, 1999], i.e., fragments of the southern (in modern coordinates) margin of the paleo-ocean. Paleozoic terrigenous and terrigenous-carbonaceous deposits compose sublatitudinal linear folds with limbs ~3–10 km along northwestern border of the Amuria block. The folds usually have asymmetric form. North limbs (toward closed Mongol-Okhotsk ocean) are steep (65–75°), south limbs have lesser slopes (25–45°). These folds contain folds of smaller scale with width down to 50 m. Faults are typical in the region (mainly as strike slip and thrust faults), and they cut many folds. As a result, in some areas Paleozoic sediments cover Middle-Late Jurassic complexes. Sediments are changed to muscovite- and quartz-bearing schists near major tectonic zones.

[6] The Paleozoic shelf deposits of the Mongol-Okhotsk paleo-ocean were studied in the Upper Amur region, where they fill the Oldoy and Gaga-Sagayan paleobasins. These extend over more than 600 km, along the northern margin of the Amurian microcontinent and are characterized by similar conditions of sedimentation. The most complete sequence is recorded within the Oldoy paleobasin, and comprises the following six formations [*Turbin*, 1994]: (1) Omutnaya formation, silurian quartz sandstones, quartzite, siltstone, grit stone and conglomerates with a thickness of 600–1000 m; (2) Bolshoy Neaver formation, lower Devonian sandstone and siltstone with a thickness in excess of 1300 m; (3) Imachi formation, lower-Middle Devonian siltstone and limestone with a thickness exceeding 500 m; (4) Oldoy formation: Middle-Upper Devonian clay shales, siltstone, tuffites and rhyolite tuffs; thickness is over

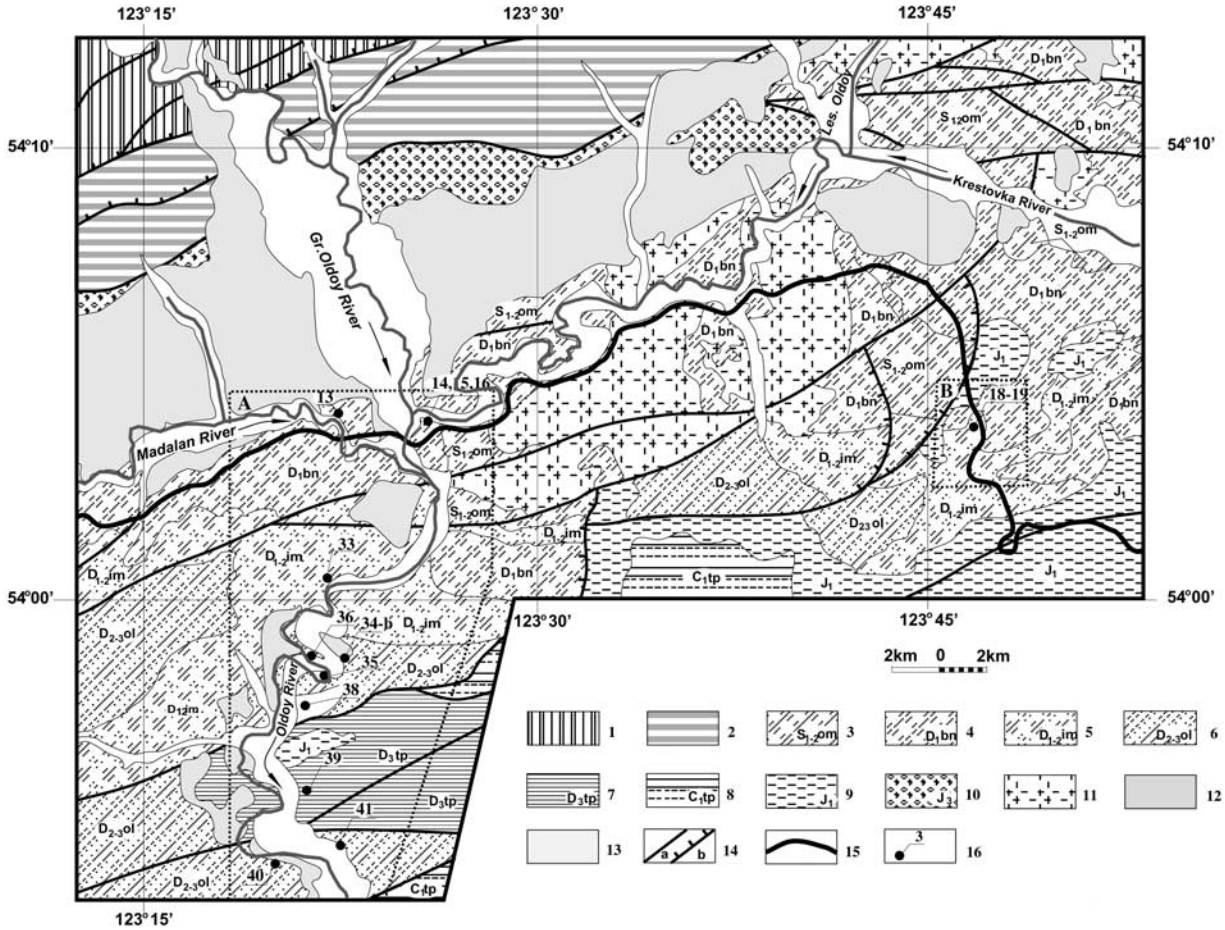

Figure 2. Geological sketch map of the Oldoy (box A) and Imachi (box B) sampling sites (modified from *Kozak et al.* [2001, 2002]. 1, Precambrian formations of the southern margin of the Siberian craton; 2, Paleozoic cilicious and volcanogenic formations and also ophiolite metagabbros of the Mongol-Okhotsk fold belt; 3–8, Paleozoic terrigenous and carbonaceous paleoshelf deposits (the Oldoy paleobasin); 3, Silurian quartzy sandstones of the Omutnaya formation; 4, Lower Devonian sandstones and limestones of the Greater Naever formation; 5, Lower-Middle Devonian siltstones, limestones of the Imachi formation; 6, Middle-Upper Devonian clay shales, siltstones of the Oldoy formation; 7, Upper Devonian sandstones, siltstones of the Teplovka formation; 8, Lower Carboniferous sandstones, siltstones of the Tipara formation; 9, Lower Jurassic marine siltstones, mudstones (the Upper Amur paleobasin); 10, Upper Jurassic conglomerates, sandstones; 11, Late Paleozoic granites; 12, Neogene loose sediments; 13, Quarternary loose sediments; 14, faults bounding (a, strike-slip, and b, thrust); 15, Trans-Siberian railway; 16, points of sampling (numbers correspond to numbers in Table 1).

1200 m; (5) Teplovka formation, upper Devonian sandstone and siltstone with a thickness in excess of 1000 m; and (6) Tipara formation, lower Carboniferous sandstone, siltstone, and limestone bands also with a thickness over 1000 m [*Turbin*, 1994].

[7] The Lower-Middle Devonian deposits comprise a rich macrofaunal complex with corals and brachiopods [see *Turbin*, 1994]. The Upper Devonian deposits are characterized by bryozoa similar to the faunal complexes of the Altai and Kuzbass territories [*Parfenov et al.*, 1999]. This similarity is particularly clear for the Early Carboniferous bryozoa communities.

[8] Sampling of the first five formations listed above was carried out in the Oldoy river basin within the Oldoy paleobasin (Figures 1 and 2). Only the Lower Carboniferous Tipara formation could not be sampled in this region. Average sampling coordinates are 123.5°E, 54.0°N (Figure 1, areas A and B). More detailed geological sketches of sampling areas A and B are given as Figure 2. Paleozoic sedimentary deposits are folded [*Freidin*, 1966; *Ol'kin et al.*, 1971]: these folds are wide and linear, gently sloping, usually symmetrical, extending in NE and east directions. Angles of dip are 30–60°.

[9] The Lower Carboniferous sedimentary deposits (the Tipara formation) were sampled on the right bank of the Zeya river, in its middle reaches, within the western part of the Gaga-Sagayan paleobasin (area C in Figures 1 and 3). Average sampling coordinates are 127.0°E, 53.6°N. Paleozoic sediments are practically everywhere overlain by Cenozoic sediments, thus forming single isolated outcrops.

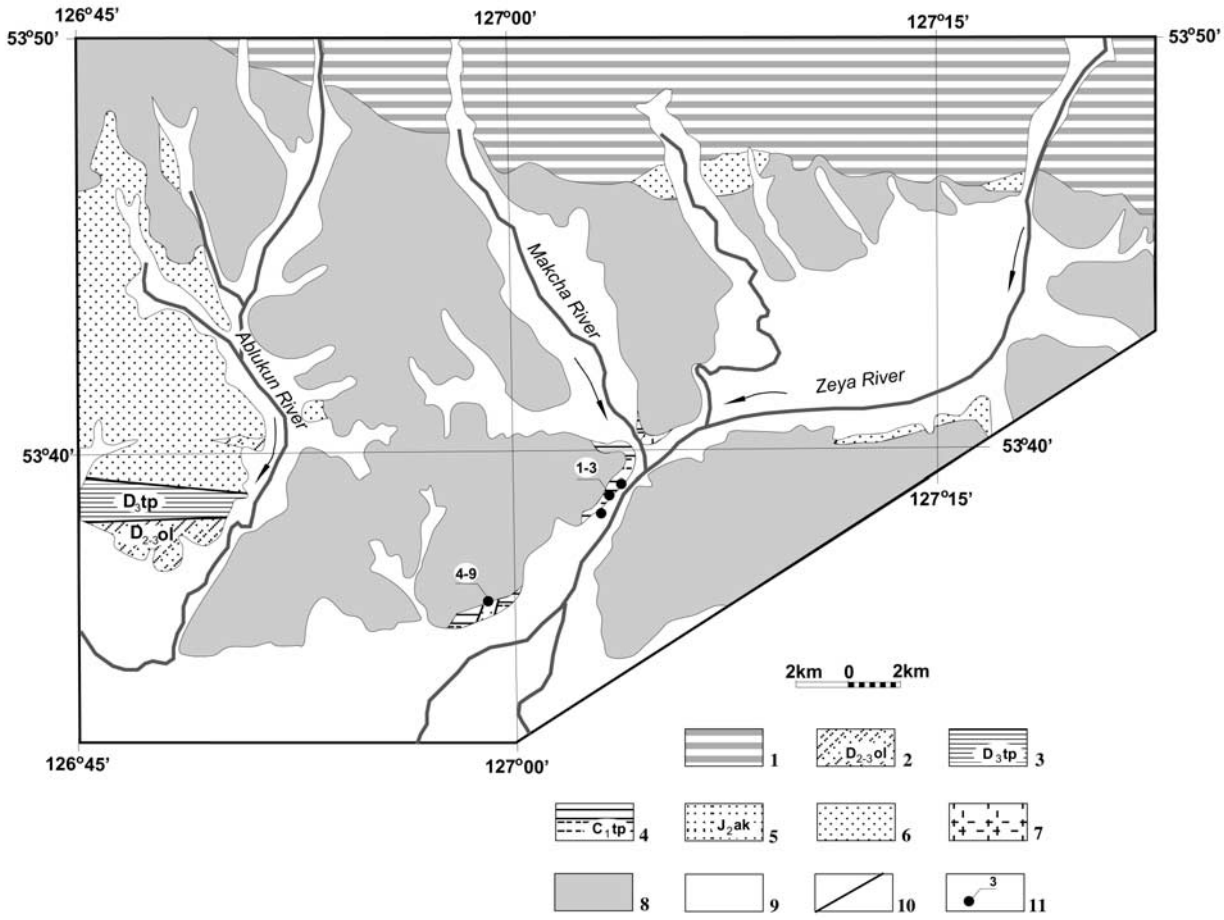

Figure 3. Geological sketch map of the Zeya (C) sampling site (modified from *Pavlenko* [1966] and *Mamontov* [1972]). 1, Paleozoic matagabbroes of the Mongol-Okhotsk fold belt; 2–4, Paleozoic terrigenous and carbonaceous paleoshelf deposits (the Gaga-Sagayan paleobasin); 2, Middle-Upper Devonian clay shales, siltstones of the Oldoy formation; 3, Upper Devonian sandstones, siltstones of the Teplovka formation; 4, Lower Carboniferous sandstones, siltstones of the Tipara formation; 5, Middle Jurassic continental sandstones and siltstones of the Ayak formation (the Zeya-Dep paleobasin); 6, Late Paleozoic granites; 7, Lower Cretaceous volcanics; 8: Neogene loose sediments; 9, Quarternary loose sediments; 10, faults; 11, points of sampling (numbers correspond to numbers in Table 1).

Paleozoic sediments are folded; folds extend in a NW direction, with dips of 50–80°, complicated by secondary folds [*Pavlenko*, 1966; *Mamontov*, 1972].

[10] The Mesozoic sedimentary deposits have been investigated within the Upper Amur and Zeya-Dep paleobasins. The former is filled with Upper Triassic, Lower and Middle Jurassic marine, and Middle Jurassic paralic deposits. Descriptions of these deposits and paleomagnetic measurements have been published earlier [*Halim et al.*, 1998a]. The sampling area is shown in Figure 1 (area D). This paleobasin is filled with Upper Triassic and Middle-Upper Jurassic deposits; in general the sequence comprises over 3000 m of Upper Triassic sandstone with siltstone bands, overlain by the following five formations: Usmanka formation: Middle Jurassic sandstones with siltstone bands (over 1100 m); Uskali formation: Middle Jurassic sandstones and siltstones with volcanics and tuff-breccia bands (over 1400 m); Ayak formation: Middle Jurassic sandstones, siltstones, lenses of conglomerates, grit stone, tuffites and tuffs (over 1500 m); Dep formation: Middle-Upper Jurassic sandstone, siltstones, argillites and carbonaceous argillites (over 1000 m); and Lower Molchan formation: Upper-Jurassic sandstones with siltstone, argillites, tuffs and coals (over 1500 m).

[11] The Mesozoic sediments of the Zeya-Dep paleobasin are deposited upon strongly deformed Paleozoic rocks. The Upper Triassic, Uskali and Usmanka formations are characterized by bivalves. The overlying Ayak, Dep and Lower Molchan formations are characterized by plant remains [*Turbin*, 1994].

[12] We sampled the Middle Jurassic sediments (Ayak formation) on the right bank of the Zeya river, in its middle reaches, within the western part of the Zeya-Dep paleobasin (area C in Figure 1). A geological sketch is shown in Figure 3. Average sampling coordinates are 127.0°E, 53.6°N. Mesozoic and Paleozoic rocks are almost everywhere overlain by Cenozoic sediments. Unlike the Devonian and Lower Carboniferous deposits of the Gaga-Sagayan

Table 1. Site-Mean Paleomagnetic Direction for the High-Temperature Component for Upper Amur Block Sedimentary Formations[a]

Site	*n*	D_g	I_g	D_S	I_S	*k*	α_{95}	N/R
Bolshoy Neaver Formation (Early Devonian, 417–395 Ma), Oldoy Paleobasin[b]								
13-1	7	138.1	−27.6	-	-	14.1	16.7	−/7
	(7d)	-	-	142.2	−9.6	17.4	14.9	
13-2	7	102.8	−44.8	-	-	18.4	14.5	−/7
	(7d)	-	-	109.7	−12.7	22.5	13.0	
13-3	4	141.9	−46.7	128.6	−16.8	40.3	14.6	−/4
	(4d)							
13-4	8	123.0	−40.1	-	-	18.5	13.2	−/8
	(8d)	-	-	112.7	−5.5	13.3	15.8	
14	6	301.2	24.8	-	-	14.3	18.3	6/−
	(6d)	-	-	302.0	−11.1	19.5	15.5	
15	6	125.0	−22.7	-	-	26.8	13.2	−/6
	(6d)	-	-	126.0	−1.0	19.5	15.5	
16	8	128.7	−43.7	-	-	25.9	11.1	−/8
	(8d)	-	-	127.6	−2.7	20.5	12.5	
Overall	7	306.0	36.3	-	-	32.4	10.8	1/6
Mean	sites	-	-	304.1	5.4	33.3	10.6	
Imachi Formation (Early-Middle Devonian, 395–381 Ma), Oldoy Paleobasin[c]								
18-1	6	163.9	−33.5	-	-	47.7	9.8	−/6
	(6d)	-	-	161.5	4.5	42.4	10.4	
18-2	8	139.4	−38.1	-	-	27.1	10.8	−/8
	(8d)	-	-	132.9	−9.9	21.4	12.2	
19-1	9	131.5	21.9	-	-	10.6	16.6	−/9
	(9d)	-	-	138.4	17.9	9.0	18.1	
19-2	6	126.8	−14.6	-	-	12.7	20.2	−/6
	(4d2cc)	-	-	118.6	−12.7	27.7	13.5	
19-3	9	149.4	−27.3	-	-	9.5	18.0	3/6
	(5d4cc)	-	-	149.2	−9.4	10.7	16.9	
19-4	8	152.6	−7.2	-	-	6.2	24.2	−/8
	(8d)	-	-	153.2	14.5	9.3	19.1	
33-1	6	325.1	20.5	-	-	14.9	18.2	6/−
	(5d1cc)	-	-	327.1	−8.2	17.7	16.6	
33-2	8	141.5	−41.7	144.4	17.1	17.5	13.6	−/8
	(8d)							
Overall	8	323.6	20.9	-	-	12.4	16.4	1/7
Mean	sites	-	-	323.3	−3.9	19.8	12.8	
Oldoy Formation (Middle-Late Devonian, 381–372 Ma), Oldoy Paleobasin[d]								
34a-1	8	150.6	−44.3	-	-	10.1	18.5	−/8
	(6d2cc)	-	-	147.7	6.0	10.4	18.3	
34a-2	7	81.3	−46.1	-	-	15.7	17.2	−/7
	(2d5cc)	-	-	109.1	−13.7	16.2	16.9	
34b	13	120.4	−51.0	-	-	7.9	15.7	−/13
	(10d3cc)	-	-	128.4	−40.8	9.0	14.7	
35	9	97.3	−45.3	112.9	−20.1	9.0	18.2	−/9
	(8d1cc)							
36	11	345.3	55.2	-	-	4.6	23.8	5/6
	(10d1cc)	-	-	313.1	18.0	8.7	16.5	
40	8	106.5	−27.6	-	-	79.5	6.3	−/8
	(8d)	-	-	114.3	−21.5	35.8	8.4	
41	13	100.3	−6.0	-	-	11.0	13.2	−/13
	(7d6cc)	-	-	100.9	−5.0	11.4	13.0	
Overall	7	114.1	−42.7	-	-	9.1	21.2	−/7
Mean	sites	-	-	120.6	−16.7	14.5	16.4	
Teplovka Formation (Late Devonian, 372–363 Ma), Oldoy Paleobasin[e]								
38	6	145.4	25.7	-	-	40.9	11.4	−/6
	(3d3cc)	-	-	142.7	−40.2	29.1	13.5	
39-1	5	153.7	−43.2	-	-	42.4	11.9	−/5
	(5d)	-	-	158.1	−29.0	44.9	11.5	
39-2	10	127.2	−28.3	135.5	−15.1	11.5	17.2	−/8
	(7d1cc)							
39-3	8	141.1	−19.9	-	-	16.9	13.9	−/8
	(8d)	-	-	144.8	−6.4	16.4	14.1	
39-4	6	126.1	−21.2	-	-	52.0	9.5	−/6
	(6)	-	-	138.5	−35.7	71.5	8.1	
Overall	5	138.1	−18.3	-	-	8.7	27.4	−/5
Mean	sites	-	-	143.9	−25.5	25.2	15.5	
Tipara Formation (Lower Carboniferous, Tournaisian-Visean, 363–333 Ma), Zeya-Dep Paleobasin[f]								
C1-01	6	187.7	−66.7	-	-	145.8	5.6	−/6

Table 1. (continued)

Site	n	D_g	I_g	D_S	I_S	k	α_{95}	N/R
	(6d)	-	-	115.7	−40.6	105.3	6.6	
C1-02	6	188.3	−64.0	-	-	373.3	3.5	−/6
	(6d)	-	-	128.1	−38.3	160.7	5.3	
C1-03	7	179.4	−66.9	-	-	73.9	7.1	−/7
	(7d)	-	-	127.1	−37.4	65.2	7.5	
C1-04	7	248.8	−64.9	-	-	98.9	6.1	−/7
	(7d)	-	-	119.0	−62.5	74.5	7.0	
C1-05	6	162.3	−41.4	-	-	21.4	14.8	−/6
	(6d)	-	-	133.0	−22.6	53.0	9.3	
C1-06	5	70.5	−55.4	-	-	30.9	14.0	−/5
	(5d)	-	-	87.3	−56.3	43.3	11.8	
C1-07	6	42.0	−44.1	-	-	127.4	6.0	−/6
	(6d)	-	-	131.8	−62.0	130.2	5.9	
C1-08	7	93.9	−63.0	-	-	267.1	3.7	−/7
	(7d)	-	-	105.0	−48.8	261.3	3.7	
Overall	8	139.5	−74.7	-	-	6.7	23.1	−/8
Mean	sites	-	-	119.8	−47.0	22.3	12.0	
		Ayak Formation (Middle Jurassic, 178–157 Ma), Zeya-Dep Paleobasin[g]						
J2-4	6	99.0	−73.0	-	-	10.5	23.0	−/6
	(3d3cc)	-	-	114.7	−45.1	24.0	14.9	
J2-5	7	39.3	−53.1	-	-	23.9	12.6	−/7
	(7d)	-	-	124.0	−67.3	17.1	15.0	
J2-6	7	87.6	−76.0	-	-	63.6	7.6	−/7
	(7d)	-	-	111.1	−49.2	65.5	7.5	
J2-7	6	186.2	−76.4	-	-	72.7	7.9	−/6
	(6d)	-	-	111.2	−52.7	89.8	7.1	
J2-8a	4	164.5	−78.4	-	-	107.3	8.9	−/4
	(4d)	-	-	149.0	−48.0	110.1	8.8	
J2-8b	5	274.0	−81.7	145.3	−54.8	35.8	13.0	−/
	(5d)							
J2-9	6	21.6	−71.8	-	-	23.6	14.1	−/6
	(6d)	-	-	107.0	−51.7	27.4	13.0	
Overall	7	71.6	−81.8	-	-	19.1	14.2	−/7
Mean	sites	-	-	122.8	−53.8	40.4	9.6	

[a] The n is number of directions and circles/study sites accepted for calculation; D (I), declination (inclination) of characteristic component of NRM in geographic (g) or stratigraphic (s) system of coordinates; k, α_{95}, precision parameter and half angle radius of the 95% probability confidence cone; N/R, number of directions of the normal/reversal polarity on sample or site levels; d or cc in means number of directions or great circles accepted for calculations. Fold test is defined with method of *Watson and Enkin* [1993].

[b] Fold test for Bolshoy Neaver formation is inconclusive (optimal concentration is found on 46.5% ± 65.7% untilting).

[c] Fold test for Imachi formation is positive (optimal concentration is found on 76.7% ± 25.4% untilting).

[d] Fold test for Oldoy formation is positive (optimal concentration is found on 78.7% ± 19.7% untilting).

[e] Fold test for Teplovka formation is close to positive (optimal concentration is found on 71.6% ± 13.4% untilting).

[f] Fold test for Tipara formation is positive (optimal concentration is found on 91.1% ± 7.2% untilting).

[g] Fold test for Ayak formation is positive (optimal concentration is found on 76.5% ± 20.5% untilting).

paleobasin, the Mesozoic sediments are much less deformed. They form gently sloping fold structures, extending in a W-E direction, with dips of 10–25° [*Pavlenko* 1966; *Mamontov*, 1972]. Fold structures in the Paleozoic and Mesozoic basins are complicated by strike-slip faults and thrusts.

[13] Paleozoic and Mesozoic pelitic and quartz-feldspar rocks comprise sericite-chlorite and clay shales, schistose sandstones, and siltstones; carbonaceous rocks are limestone and marble. Silicification is widely developed, but hornfels are rare. This required thorough selection of sampling sites with minimal secondary rock alteration. We selected the localities with absence of or minimal secondary changes.

[14] In order to better constrain the evolution of the Mongol-Okhotsk ocean, we sampled seven formations of paleontologically dated Silurian to Middle Jurassic sedimentary formations from the southern side of the Mongol-Okhotsk suture (Figure 2), but Silurian sediment magnetization is very week, and we do not discuss Omutnaya formation further. All sampling sites are listed in stratigraphic order in Table 1, from lower to upper part of each formation.

3. Paleomagnetic Methods

[15] Samples were subjected to stepwise thermal and alternating magnetic field (AF) demagnetizations in the paleomagnetic laboratories of the East Siberian Research Institute and Institute of Geochemistry (Irkutsk, Russia), and of the Institut de Physique du Globe de Paris (France). All (8 cm^3) cubic samples were extracted from hand blocks, which had been sampled in the field. Usually, one or two samples were analyzed in each block.

[16] In Irkutsk, samples were heated and cooled in a nonmagnetic oven placed within a triple μ-metal shield (developed by V. P. Aparin, Institute of Physics, Krasnoyarsk). In the center of the oven, the residual field is about 8nT. Measurements of remanent magnetization were made with a JR-4 spinner magnetometer. Magnetic suscept-

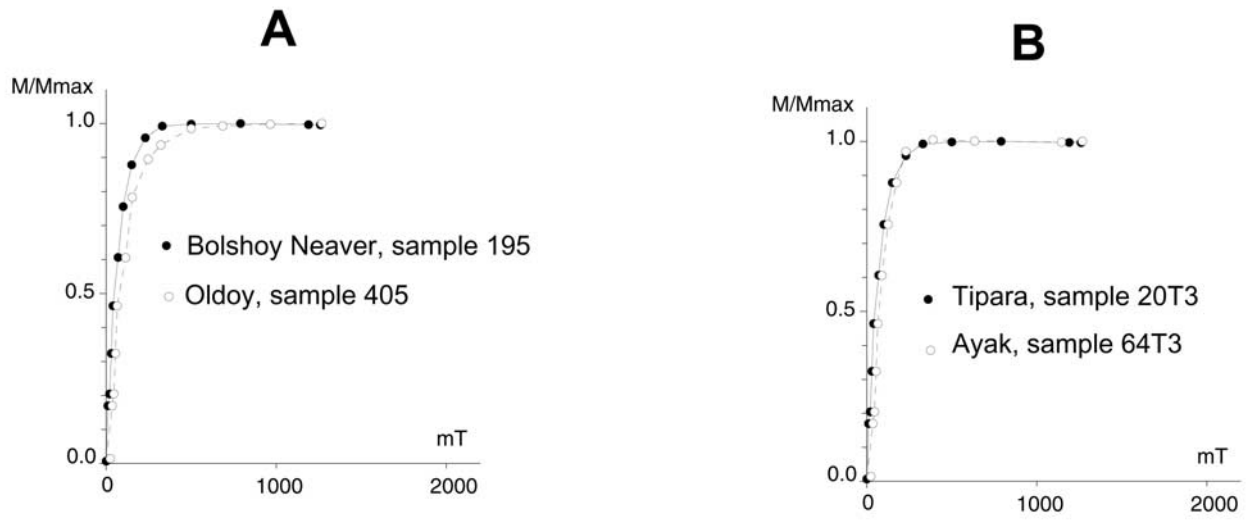

Figure 4. IRM acquisition in fields up to 1.2T showing the presence of low-coercivity magnetic mineral (possibly magnetite) for (a) Devonian and (b) Carboniferous and Jurassic samples.

ibility was measured with a KLY-2 Kappa-bridge, manufactured in Czechoslovakia [*Jelinek*, 1966, 1973].

[17] About 80% of the studied samples were measured with a cryogenic magnetometer (2G Superconducting Rock Magnetometer) in Paris. In order to compare results, 10% of the samples from the same blocks were demagnetized in both Paris and Irkutsk. The two sets of laboratory results are virtually identical. Thermal demagnetizations were made with Schonstedt oven, installed in the magnetically shielded room at IPGP (total field in cooling region is about 5nT). Demagnetization by AF turned out to be ineffective for these sediments, which is why most samples were thermally demagnetized. Changes in magnetic mineralogy during thermal demagnetization were monitored by measurements of magnetic susceptibility after each heating step.

[18] Changes in the intensity and direction of remanent magnetization vectors during demagnetization experiments were analyzed using orthogonal vector end-point projections [*Zijderveld*, 1967]. Magnetic component directions were identified using principal component analysis (PCA) [*Kirschvink*, 1980], or remagnetization great circles method [*Halls*, 1976] with sector constraints [*McFadden and McElhinny*, 1988]. Site-mean directions were determined using *Fisher*'s [1953] statistics or, in the case of combined directional data and remagnetization circles, using *McFadden and McElhinny*'s [1988] statistics. Data were processed using the paleomagnetic data treatment softwares of *Enkin* [1990] and J.-P. Cogné (free software Paleo Mac) and the Opal software [*Vinarsky et al.*, 1987].

4. Paleomagnetic Results

4.1. Early Devonian Bolshoy Neaver Formation (417–395 Ma) of the Oldoy Paleobasin

[19] The isothermal remanent magnetization (IRM) acquisition curves (Figure 4) show that magnetite is the most likely carrier of remanence in all studied localities. During thermal demagnetization of the samples, we separated two different components of NRM (Figure 5). A low-temperature component (LTC) is removed after heating up to 250–300°C. The *Fisher* [1953] average of this component in geographic coordinates is D_g = 14.5°, I_g = 75.2° (k_g = 13.4, α_{95} = 17.1°, n = 7 sites).

[20] This component is close to the present-day geomagnetic field (D = 348.5°, I = 71°) in geographic coordinates. After this LTC, the high-temperature component (HTC) unblocks between 450°C and 590°C (Figure 5). This temperature range, together with the low coercivity evidenced by IRM acquisition curves, shows that magnetite is the most likely carrier of this component. This HTC could be isolated in only 50% of the samples. About 50% of the rest of the samples displayed remagnetization great circles, and the *McFadden and McElhinny* [1988] statistics was used to determine site-mean directions of HTC for both directions and great circles with sector constraints. About 40% of samples from five sites (from 13-1 to 14) have intermediate component, as might be seen in Figure 5. The component has always negative direction but too scattered to provide a statistically significant value.

[21] For HTC, the fold test of *Watson and Enkin* [1993] gives an optimum degree of untilting (50 percentile, 1000 trials) at 46.5% (with 95% confidence limits at −2.8 and 128.5%). The fold test is therefore inconclusive. The fold test using the *McElhinny* [1964] method is also inconclusive at the 95% confidence level (ks/kg = 1.03, n = 7 sites). We cannot discuss the possibility of a synfolding remagnetization. It is known that the age of folding in the region might be linked with closing of the Mongol-Okhotsk ocean and postcollisional shortening and rotations of blocks (from Late Jurassic to Cenozoic) [*Zonenshain et al.*, 1990; *Sorokin*, 1992]. Both paleomagnetic polarities have been recovered (normal polarity in one site and reversed polarity in the other six). However, the reversal test [*McFadden and Lowes*, 1981; *McFadden and McElhinny*, 1990] is not statistically significant (classification "I" of *McFadden and McElhinny* [1990], due to the large critical value of 29.1° obtained for this population). Yet, on the basis of the presence of both polarities, we suggest that the average HTC direction is the

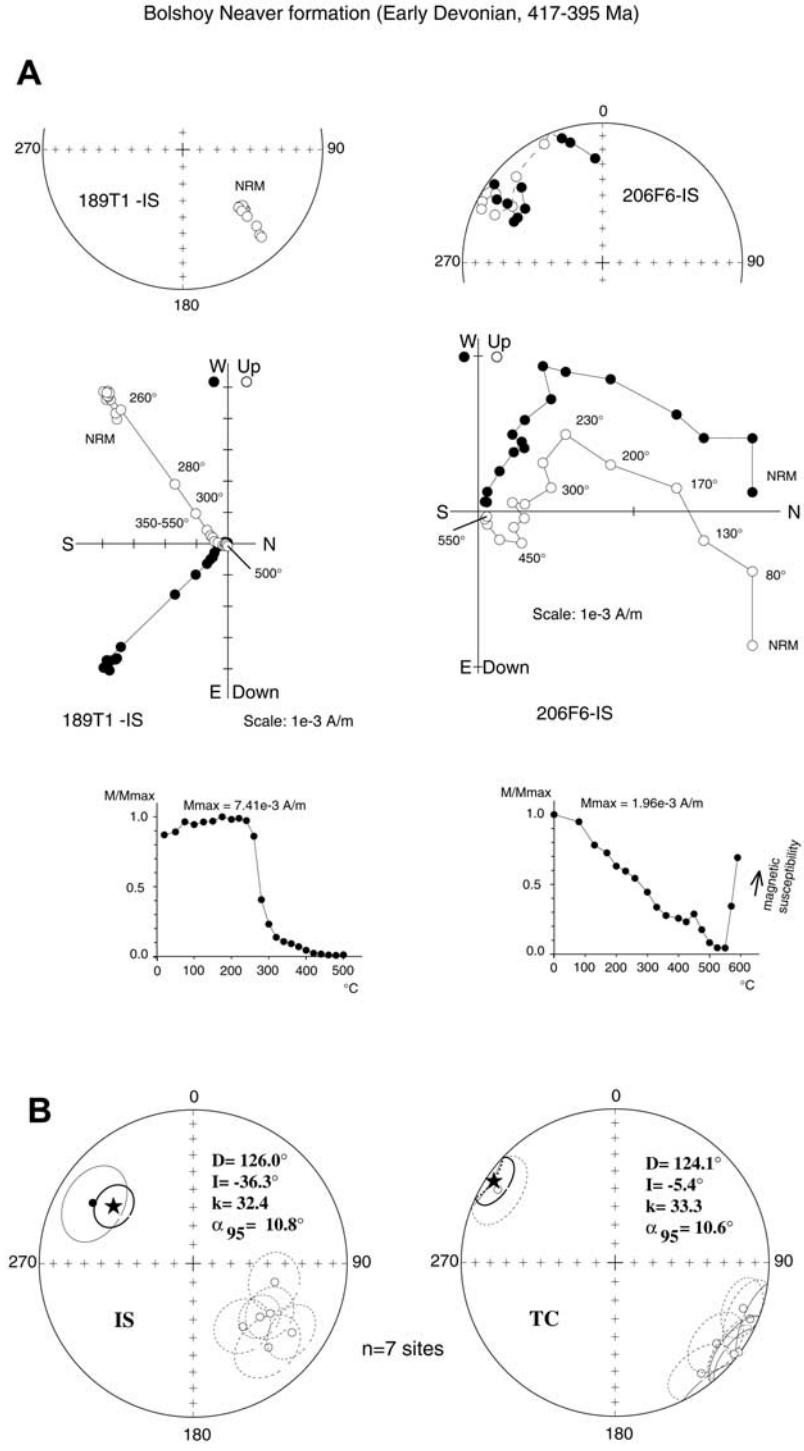

Figure 5. (a) Results of thermal demagnetization and (b) equal-area projections of site-mean directions of high-temperature component for Bolshoy Neaver formation (Early Devonian) samples. Typical equal-area projections illustrating (top) demagnetization paths during experiments, (middle) thermal demagnetization orthogonal vector plots in situ coordinates [*Zijderveld*, 1967], and (bottom) magnetic intensity decay curves. Solid (open) symbols in orthogonal plots: projections onto the horizontal (vertical) plane; temperature steps are indicated in degrees Celsius. Arrows near intensity decay curves show increasing magnetic susceptibility. (b) Site-mean directions (stars) are shown with their circles of 95% confidence shown in situ (IS) and tilt-corrected (TC) coordinates. Solid (open) symbols: downward (upward) inclinations. Star, formation mean directions.

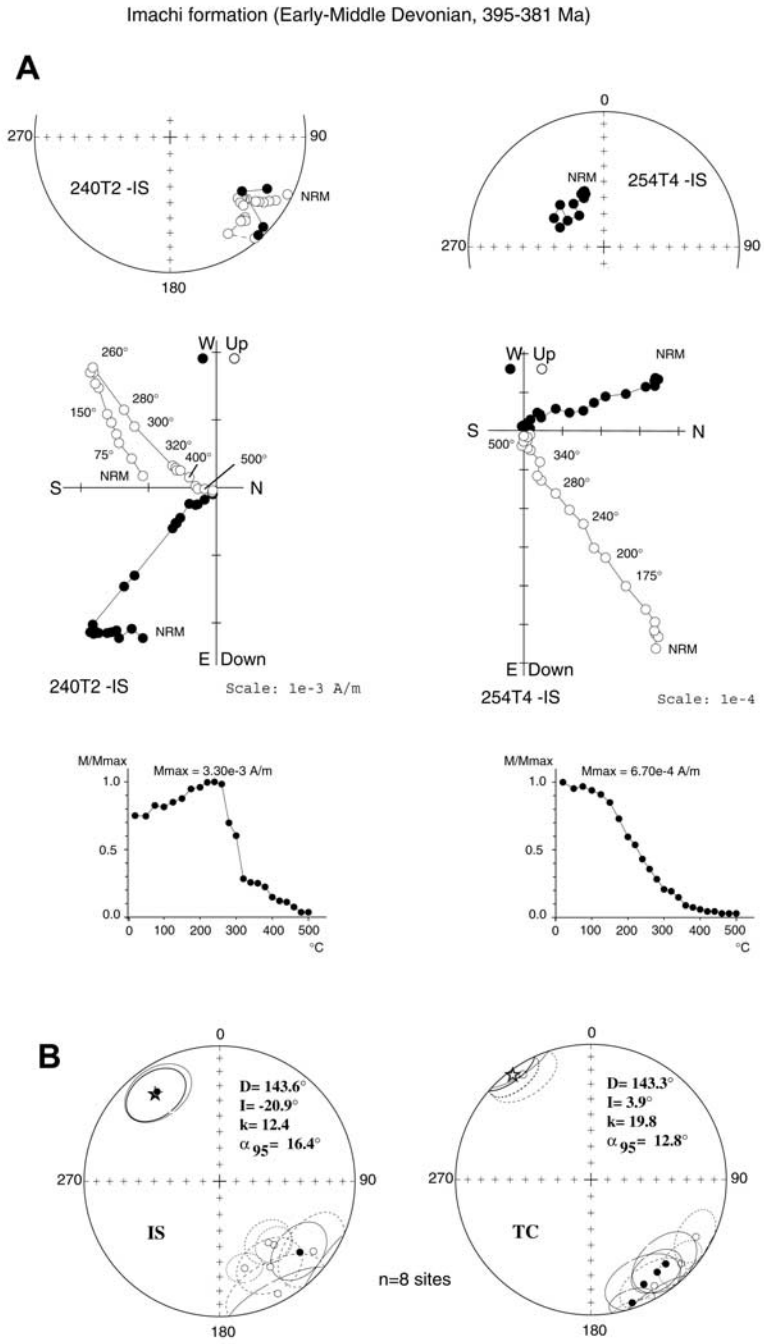

Figure 6. (a) Results of thermal demagnetization and (b) equal-area projections of site-mean directions of high-temperature component for Imachi formation (Early-Middle Devonian) samples. Abbreviations are the same as in Figure 5.

primary Early Devonian magnetization of this formation. The average tilt-corrected direction is $D_S = 304.1°$, $I_S = 5.4°$ ($k_S = 33.3$, $\alpha_{95} = 10.6°$, $n = 7$ sites; Table 1).

4.2. Early-Middle Devonian Imachi Formation (395–381 Ma) of the Oldoy Paleobasin

[22] Two components were isolated in 8 sites from the Early-Middle Devonian Imachi formation (Figure 6). The LTC could be seen in temperature intervals from NRM to 150–250°C. The LTC concentration parameter maximizes at 4.8% unfolding [*McElhinny*, 1964] and is negative at the 99% confidence level, with the ratio of precision parameters $k_g/k_S = 3.6$. The same holds for the *Watson and Enkin* [1993] test. The in situ Fisher average is $D_g = 11.7°$, $I_g = 78.6°$ ($k_g = 24.7$, $\alpha_{95} = 14.4°$, $n = 7$ sites). This direction is close to the present-day geomagnetic field in the region ($D = 348.5°$, $I = 71°$). We again interpret the LTC as a postfolding Cenozoic overprint.

[23] For the HTC, the fold test of *McElhinny* [1964] is inconclusive (77.0% untilting at 95% probability; k_S/k_g = 1.6, n = 8 sites). The optimal concentration is found on 76.7% ± 25.4% untilting (95% confidence interval using the method of *Watson and Enkin* [1993]): the remanence may therefore be pretilting. We therefore assume that the average direction of the HTC is the primary Early-Middle Devonian magnetization of the Imachi formation. The presence of two antipodal polarities is consistent with this, though not statistically significant at the site level. The average tilt-corrected direction is D_S = 323.3°, I_S = −3.9° (k_S = 19.8, α_{95} = 12.8°, n = 8 sites; Table 1). We note that the HTC directions for the early Devonian Bolshoy Neaver and early-middle Devonian Imachi formations are very close to each other.

4.3. Middle-Late Devonian Oldoy Formation (381–372 Ma) of the Oldoy Paleobasin

[24] Thermal demagnetization isolates two components in the Middle-Late Devonian Oldoy formation (Figure 7). The LT component (300–330°C) is directed mostly north and down at low temperatures. The fold test of *McElhinny* [1964] is negative with maximum concentration parameter at 7.4% unfolding at 95% probability (k_g/k_S = 3.8, n = 7 sites), and so is that of *Watson and Enkin* [1993] (−7.3%, with 95% confidence limits at −29.1 and 17.0%). The average in situ direction is D_g = 31.2°, I_g = 65.7° (k_g = 31.2, α_{95} = 11.0°, n = 7 sites) and is probably a Cenozoic overprint.

[25] Above 300–330°C, the HTC decays toward the origin of the demagnetization diagrams. The best estimate for the amount of unfolding is 78.4% (95% probability; k_S/k_g = 1.6, n = 7 sites) [*McElhinny*, 1964]. The fold test of *Watson and Enkin* [1993] gives an optimum untilting at 78.7% (95% confidence limits at 58.7 and 98%), close enough to 100% that remanence can be considered pretilting. We therefore assume that the average HTC direction is the primary Middle-Late Devonian magnetization of the Oldoy formation. All directions of the formation have reversed polarity except for site 36 where two polarity intervals were found in different stratigraphic levels (5 samples below have normal polarity and 6 samples above are reversed). The average tilt-corrected reversed direction is D_S = 120.6°, I_S = −16.7° (k_S = 14.5, α_{95} = 16.4°, n = 7 sites; Table 1).

4.4. Late Devonian Teplovka Formation (Middle-Late Devonian, 372–363 Ma) of the Oldoy Paleobasin

[26] Thermal demagnetization yields the separation of two magnetization components (Figure 8). A low unblocking temperature component with northerly declinations and downward inclinations (in geographic coordinates) is removed below 350–400°C. The contribution of this component to the total NRM may represent more than 70% of the total intensity. The fold test of *McElhinny* [1964] is indeterminate with maximum concentration parameter at 63.8% unfolding (kg/ks = 0.8). The in situ Fisherian average of this component lies at D_g = 38.7°, I_g = 78.7° (k_g = 4.2, α_{95} = 14.9°, n = 29 samples) and is close to the present field in the region, and thus this component is most likely a recent overprint.

[27] After removal of the LTC, the HTC is isolated in the temperature interval between 350–400°C and 560–600°C. The fold test of *McElhinny* [1964] has 72% of untilting with k_S/k_g = 2.9. The fold test of *Watson and Enkin* [1993] gives optimum untilting at 71.6% (95% confidence limits at 57.9 and 84.6%) and is not so close to 100% as for other formations. The average tilt-corrected direction is D_S = 323.9°, I_S = 25.5° (k_S = 25.2, α_{95} = 15.5°, n = 5 sites; Table 1). To indicate that remanence is likely pretilting, we note that this direction is very close to other Paleozoic directions of the study. Also this direction is clearly far from Cenozoic and present-day overprint directions.

4.5. Tournaisian-Visean Tipara Formation (Lower Carboniferous, 363–333 Ma) of the Zeya-Dep Paleobasin

[28] The results of thermal demagnetization of NRM are shown in Figure 9. The orthogonal vector plots clearly exhibit two components of magnetization. A LTC is demagnetized by 270–400°C. The *McElhinny* [1964] fold test is negative (12.1% maximum untilting; k_g/k_S = 4), confirmed by the fold test of *Watson and Enkin* [1993] (12.2%, with 95% confidence limits at 3.1 and 21.8%). The average in situ direction is D_g = 46.4°, I_g = 84.4° (k_g = 31.3, α_{95} = 10.1°, n = 8 sites), and likely a Cenozoic overprint.

[29] The HTC is removed by 580–600°C. The fold test of *McElhinny* [1964] has 91.3% of untilting for the component at 95% of probability (k_S/k_g = 3.3, n = 8 sites), and that of *Watson and Enkin* [1993] gives optimum untilting at 91.1% (with 95% confidence limits at 84.3 and 98.6%): remanence is likely pretilting. We therefore assume that the average HTC direction is the primary Tournaisian-Visean magnetization of the Tipara formation. The average tilt-corrected direction is D_S = 299.8°, I_S = 47.0° (k_S = 22.3, α_{95} = 12.0°, n = 8 sites).

4.6. Middle Jurassic Ayak Formation of the Zeya-Dep Paleobasin

[30] Thermal demagnetization of the samples (Figure 10) isolates two magnetization components. A low-temperature component (LTC) is easily removed after heating up to 250–475°C and makes up ~10–25% of the total NRM intensity. This component coincides with the present-day geomagnetic field in geographic coordinates. The *Fisher* [1953] average of this component in geographic coordinates is D_g = 91.0°, I_g = 85.6° (k_g = 18.6, α_{95} = 14.4°, n = 7 sites). The two fold tests [*McElhinny*, 1964; *Watson and Enkin*, 1993] are negative. Again, the LTC is interpreted as a Cenozoic overprint.

[31] The HTC unblocks between 450° and 590°C. This temperature range, together with the low coercivity minerals evidenced by the IRM acquisition curves show that magnetite is the most likely carrier of this component. This HTC could be isolated in most samples. Only 3 samples of site J2-4 displayed remagnetization great circles, and *McFadden and McElhinny* [1988] statistics was used to determine site-mean directions.

[32] The *Watson and Enkin* [1993] fold test gives optimum untilting at 76.5% (with 95% confidence limits at 56.5 and 97.5%), close to 100%, indicating that remanence is likely pretilting. The *McElhinny* [1964] fold test is inconclusive at 95% probability (ks/kg = 2.1, n = 7 sites). We assume that the average HTC direction is the primary Middle Jurassic magnetization of this formation. The aver-

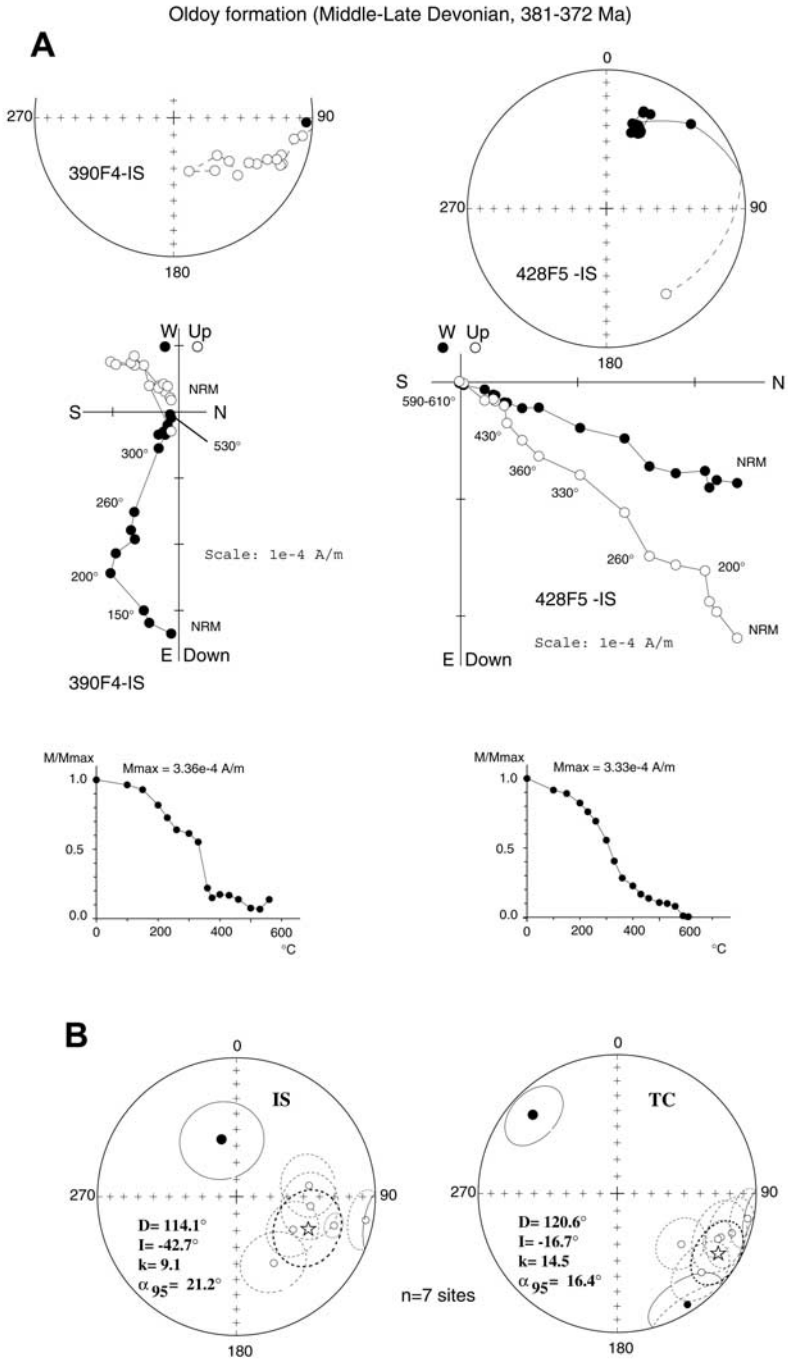

Figure 7. (a) Results of thermal demagnetization and (b) equal-area projections of site-mean directions of high-temperature component for Oldoy formation (Middle-Late Devonian) samples. Abbreviations are the same as in Figure 5.

age tilt-corrected direction is $D_S = 122.8°$, $I_S = -53.8°$ ($k_S = 40.4$, $\alpha_{95} = 9.6°$, $n = 7$ sites; Table 1).

5. Discussion

5.1. Paleomagnetic Poles for Devonian, Early Carboniferous, and Middle Jurassic

[33] Paleomagnetic analysis allows the separation of (at least) two magnetization components in each of the six formations studied. The LTC shows negative fold tests in four formations (Early-Middle Devonian Imachi, Middle-Late Devonian Oldoy, Early Carboniferous Tipara, and Middle Jurassic Ayak formations), and inconclusive fold tests in the other two (Early Devonian Bolshoy Neaver and Late Devonian Teplovka formations). In each case, the LTC (in geographic coordinates) is close to the present-day geomagnetic field direction at the sampling localities. The overall LTC mean for all localities is $D_g = 39.5°$, $I_g = 79.7°$

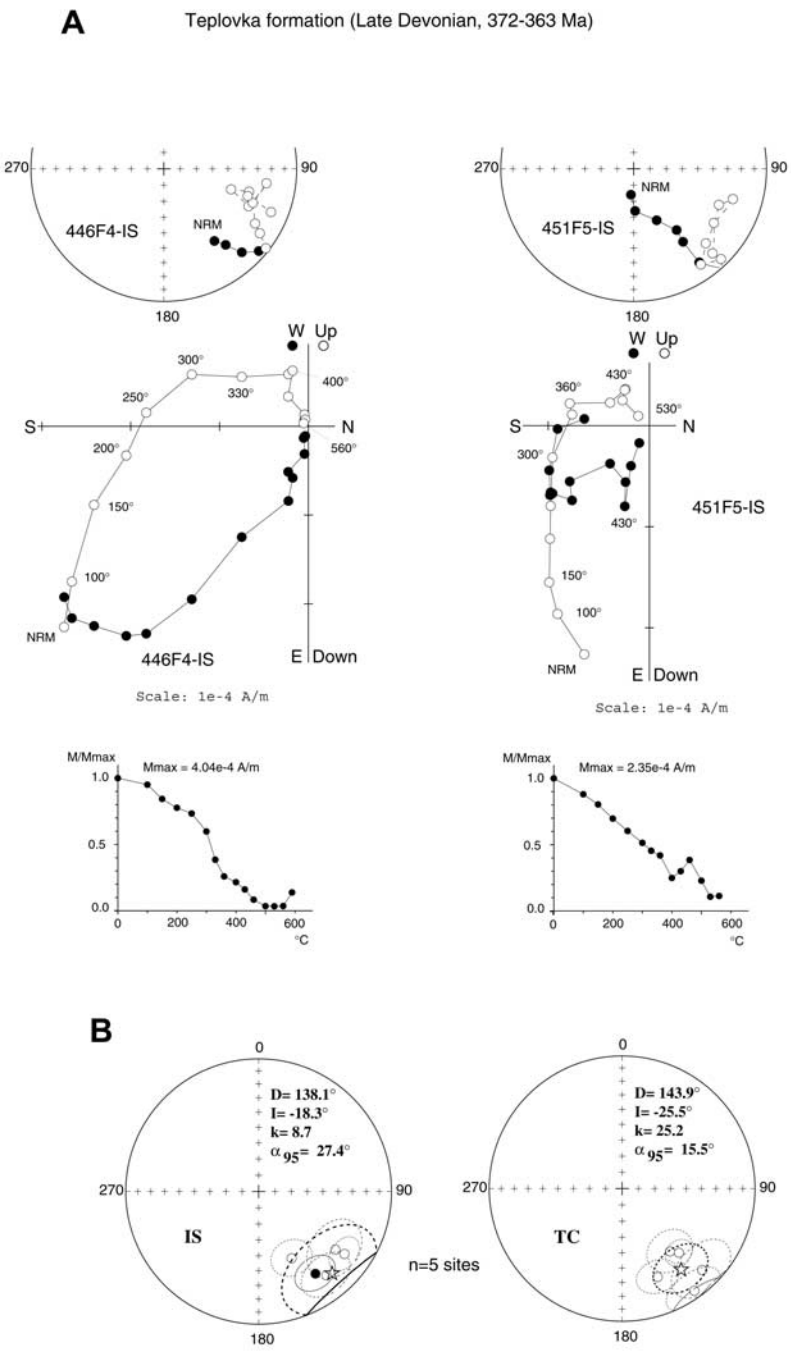

Figure 8. (a) Results of thermal demagnetization and (b) equal-area projections of site-mean directions of high-temperature component for Teplovka formation (Late Devonian) samples. Abbreviations are the same as in Figure 5.

(k_g = 16.3, α_{95} = 5.6°, n = 42 sites; Figure 11). This is significantly different from the present-day geomagnetic field (D = 348.5°, I = 71°) in the studied region. Yet both the *McElhinny* [1964] and *Watson and Enkin* [1993] fold tests are negative at 95% probability (maximum untilting at 20.3%, k_g/k_S = 2.1). The paleopole of the LTC in in situ coordinates (66.2°N, 156.1°E; dp/dm = 10.2°/10.7°) is close to the overprint pole for Jurassic-Triassic rocks in the region (76.8°N, 152.2°E; A_{95} = 4.2°) already found by *Halim et al.* [1998a] (Figure 12). We therefore assume that the same interpretation holds and that the LTC is more likely a Cenozoic (~50 Ma) remagnetization. Although the upper Jurassic–lower Cretaceous (~150 Ma) remagnetization is not excluded.

[34] A HTC could be isolated in most samples. This HTC was not always easy to separate from the LTC because of overlapping unblocking temperature spectra and/or weak intensity. In some cases, we had to use remagnetization circles with sector constraints [*McFadden and McElhinny*,

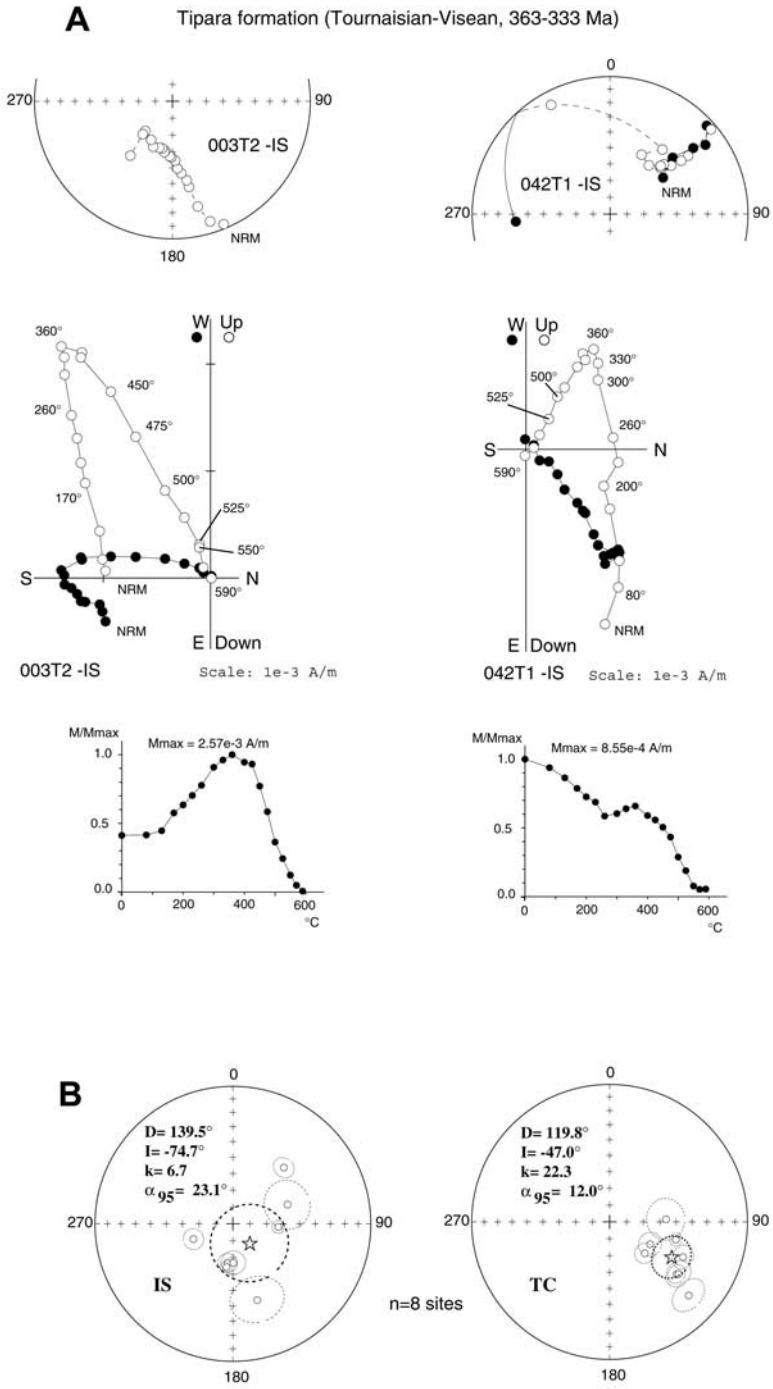

Figure 9. (a) Results of thermal demagnetization and (b) equal-area projections of site-mean directions of high-temperature component for Tipara formation (Middle-Late Devonian) samples. Abbreviations are the same as in Figure 5.

1988]. The fold test of *Watson and Enkin* [1993] is positive for four formations out of six (Early-Middle Devonian Imachi, Middle-Late Devonian Oldoy, Early Carboniferous Tipara, and Middle Jurassic Ayak formations). The fold test for Late Devonian Teplovka formation is close but not fully positive. The arguments in favor of primary direction of the HTC for that formation are that Teplovka pole is close to other Paleozoic formation poles, and far from present-day overprint directions. The *McElhinny* [1964] fold test is positive for the same four formations and is inconclusive at the 95% probability level for the early Devonian Bolshoy Neaver formation. Finally we note that the formation mean HTC is not parallel to the Cenozoic or present-day geomagnetic field direction in any of the six studied formations

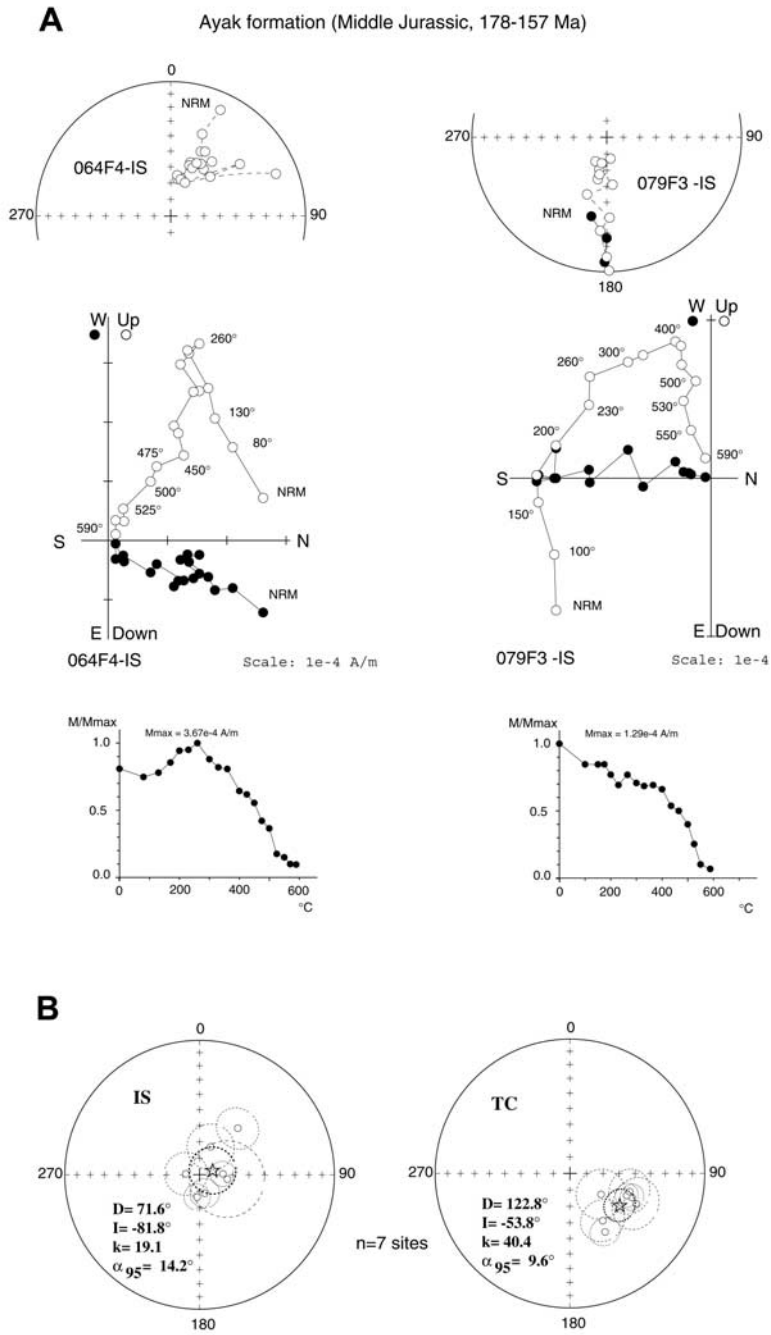

Figure 10. (a) Results of thermal demagnetization and (b) equal-area projections of site-mean directions of high-temperature component for Ayak formation (Middle Jurassic samples. Abbreviations are the same as in Figure 5.

and that most have reversed polarity. Both normal and reversed polarities could be identified in three localities (early Devonian Bolshoy Neaver, early-middle Devonian Imachi, and Middle-Late Devonian Oldoy formations). The stratigraphic sequence of polarity changes is listed in Table 1, from older to younger sites (lower sites have lower numbers). The average directions of the Devonian formations are close to each other. Based on the positive fold tests and two polarities in the Devonian, and positive fold test for Early Carboniferous and Middle Jurassic, we have assumed that these HTC are the primary paleomagnetic directions of the 6 studied formations. The corresponding paleopoles, computed after tilt-correction, are listed in Table 2, along with selected paleopoles from the literature for Siberia and Amuria (south of the Mongol-Okhotsk suture). In the following, we discuss these paleopoles with respect to the reference apparent pole wander path (APWP) of Eurasia [*Besse and Courtillot*, 1991, 2002; *Van der Voo*, 1993] and of North China Block (NCB) [*Zhao et al.*, 1996; *Enkin et al.*, 1992; *Gilder and Courtillot*, 1997].

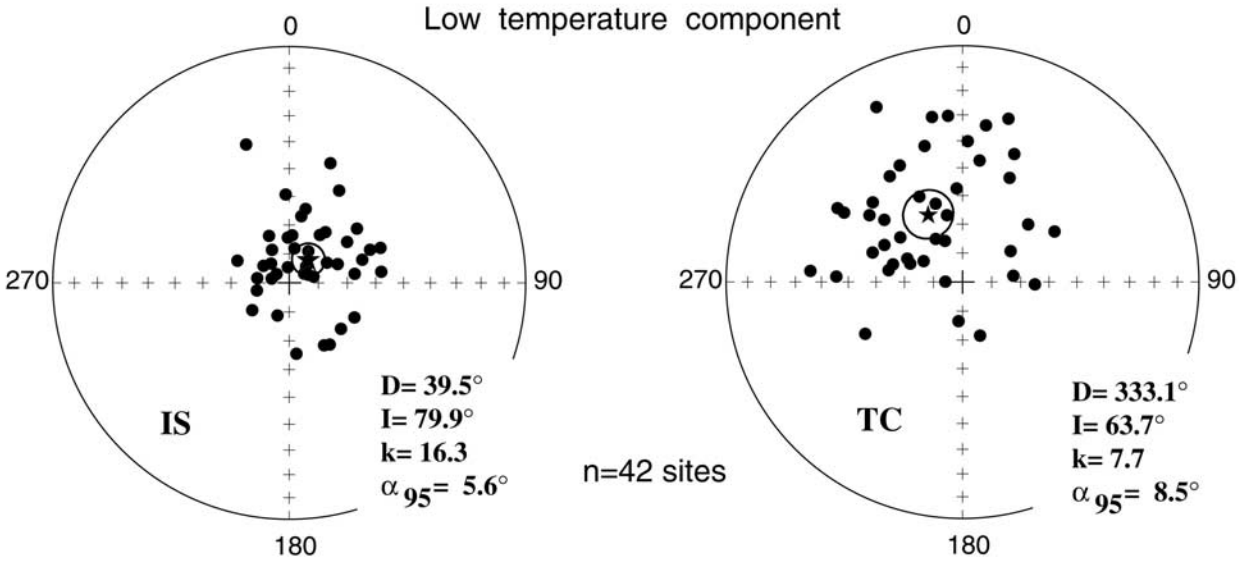

Figure 11. Equal-area projection of the low-temperature component site-mean directions (left) before and (right) after tilt correction.

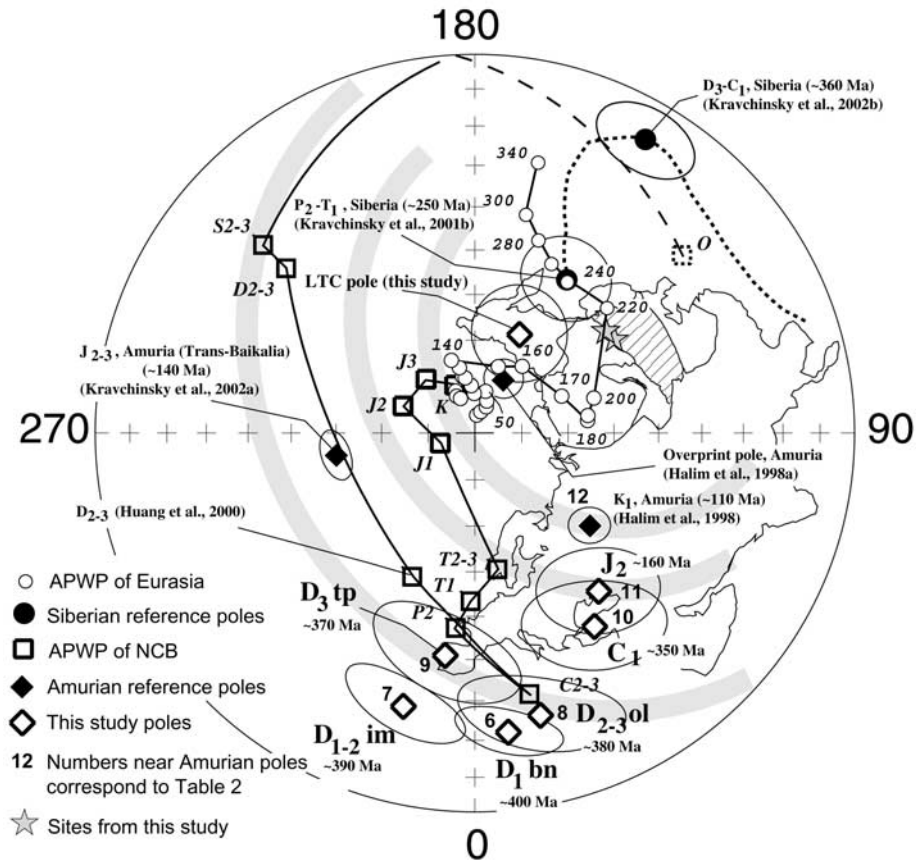

Figure 12. Equal-area projection of the northern hemisphere with the Devonian (Bolshoy Neaver (D_1bn), Imachi (D_{1-2}im), Oldoy (D_{2-3}ol), and Teplovka (D_3tp) formations), Early Carboniferous (Tipara formation (C_1)), and Middle Jurassic (Ayak formation (J_2)) from the present study (large dots with *dp*/*dm* ellipses of confidence) and from the literature [*Halim et al.*, 1998a; *Kravchinsky et al.*, 2002a, 2002b]. Small open dots, Eurasian APWP [*Besse and Courtillot*, 1991; *Van der Voo*, 1993] with ages indicated in Ma. Open diamonds, North China Block (NCB) APWP [*Enkin et al.*, 1992, *Gilder and Courtillot*, 1997; *Zhao et al.*, 1996] Grey curves are the small circles passing through this study poles and centered on site location (gray stars).

Table 2. Paleozoic and Mesozoic Paleopoles From This Study and Selected Paleopoles From Siberia and Amuria Regions[a]

Pole	Block/Area	Formation	Age	Site		Paleopole		*dp/dm* (A_{95})	*N*	Paleolat.	References
				Lat	Lon	Lat	Lon				
			North of Mongol-Okhotsk suture (Siberian Continent)								
1	Khilok	Alentuy	P2	50.8	107.2	63.1	151.0	13.8/15.0	15S	63.8	*Kravchinsky et al.* [2002a]
2	Lena river	sediments, no details	T2-3-J1	72.6	124.7	47	129	4/16	26s	64.3	*Pisarevsky* [1982]
3	Ilek	Ilek group	J2-3	56.5	89.5	74	135	10.4/11.2	101s	65.3	*Pospelova* [1971]
4	Mogzon	Badin	J3	51.8	112.0	64.4	161.0	6.7/7.3	9S	62.1	*Kravchinsky et al.* [2002a]
5	Kondersky	intrusives, sediments	J + K	57.7	134.6	75	163	10.4/10.9	34s	69.7	*V. E. Pavlov* [1993][c]
			South of Mongol-Okhotsk suture (Upper Amur region of Amuria Block)								
6[b]	Oldoy	Bolshoy Neaver	D1 (417–395)	54.0	123.5	21.6	6.3	5.3/10.6	7S	2.7	this study
7[b]	Oldoy	Imachi	D1-2 (395–381)	54.0	123.5	26.3	345.3	6.4/12.8	8S	−2.0	this study
8[b]	Oldoy	Oldoy	D2-3 (381–372)	54.0	123.5	24.6	12.9	8.7/16.9	7S	8.5	this study
9[b]	Oldoy	Teplovka	D3 (372–363)	54.0	123.5	40.5	352.4	9.0/16.7	5S	13.4	this study
10[b]	Zeya-Dep	Tipara	C1, Tournaisian-Visean (363–333)	53.58	127.0	39.8	31.6	10.0/15.5	8S	28.2	this study
11[b]	Zeya-Dep	Ayak	J2 (178–157)	53.58	127.0	46.0	37.9	9.4/13.4	7S	34.3	this study
12[b]	Upper Amur	Taldan	K1 (97–146)	53.8	124.5	58.3	51.0	3.8/4.6	14S	50.8	*Halim et al.* [1998a]
			South of Mongol-Okhotsk Suture (Trans-Baikal Region of Amuria Block)								
13	Chiron	Karashibir	C2 (320–296)	51.53	115.39	10.2	186.2	14.8	8S	19.9	*Xu et al.* [1997]
14[b]	Mongolia	-	C3	46.2	107.4	37.5	320.1	10.4	5L	−1.3	*Pruner* [1992]
15	Chiron	Zhipkhoshin	P1	51.53	115.39	33.8	207.8	26.3	5S	24.4	*Xu et al.* [1997]
16[b]	Mongolia	-	P1	47.8	107.1	44.8	335.1	11.6	4L	11.7	*Pruner* [1992]
17[b]	Borzja	Belektuy	P2	50.65	116.88	8.3	183.9	9.5/16.2	14S	20.9	*Kravchinsky et al.* [2002a]
18[b]	Unda-Daya (in-situ)	Shadaron	J2-3	51.5	117.5	68.6	261.8	3.4/4.9	8S	33	*Kravchinsky et al.* [2002a]

[a] Lat (Lon), latitude (longitude) of sampling sites or paleomagnetic poles; A_{95}, radius of the 95% confidence circle of the virtual paleomagnetic pole; *dp/dm*, semiaxes of the confidence circle of paleomagnetic pole; Paleolat., paleolatitude; *N*, number of localities or sites (L), samples (s) or sites (S) used to determine pole.

[b] Poles accepted for reconstructions in Figures 11 and 12.

[c] Paleomagnetic directions and paleomagnetic pole positions: Data for the former USSR, unpublished catalogue, VNIGRI Institute, St. Petersburg, Russia, 1993.

[35] In Figure 12, we show all poles found in the present study, together with some Middle-Late Jurassic and early Cretaceous poles of Amuria [*Halim et al.*, 1998a; *Kravchinsky et al.*, 2002a], and related APWPs of Eurasia and north China. The Late Devonian–Early Carboniferous and Late Permian–Early Triassic poles for Siberia are from *Kravchinsky et al.* [2002b]. Then, from 240 Ma, we use the APWP of Eurasia [*Besse and Courtillot*, 1991; *Van der Voo*, 1993] under the assumption that final closing of the Uralian paleo-ocean occurred before this time [*Zonenshain et al.*, 1990]. We included the poles from the Oldoy, Zeya-Dep and Upper Amur areas (poles 6–12 from Table 2). The poles of the Trans-Baikal region and eastern Mongolia (poles 13–18, Table 2) might be used for paleolatitude calculations, but not for constraining the APWP, since these poles are strongly rotated relative to each other and to other areas in Amuria [*Kravchinsky et al.*, 2002a]. On the basis of selected poles from Table 2, we can see that large relative rotations took place between poles of NCB and Amuria. Small circles of rotation, connected to relevant poles with respect to their sampling localities are shown in gray in Figure 12 for the Middle-Late Devonian, Middle Jurassic, and Early Cretaceous.

[36] The Middle-Late Devonian Oldoy formation paleopole (pole 8 in Figure 12 and Table 2) is rotated counterclockwise with respect to the reference Middle-Late Devonian pole of NCB (34.2°N, 228.7°E, A_{95} = 8.8° [*Zhao et al.*, 1996]) (Figure 12); the corresponding rotation angle is $\Delta D = 93.7° \pm 9.3°$, whereas the paleolatitude difference is negligible, at $\Delta\lambda = 5.7° \pm 7.0°$. We suggest that the rotation time was likely post-Early Cretaceous, i.e., final closing of Mongol-Okhotsk ocean. We propose, following *Halim et al.* [1998a], that the most significant rotations of Amurian blocks occurred at about this time. Indeed the early Cretaceous pole of *Halim et al.* [1998a] is rotated (Figure 12), whereas the ~50 Ma overprint pole is not (relative to the APWP of Eurasia). We have also plotted the paleolatitudes for Siberia, north China and Amuria for last 450 Myr (Figure 13). The paleolatitude calculations were made for a reference point on (the present) Mongol-Okhotsk suture at 54°N, 124°E. This point is located on the present-day boundary between Siberia and Amuria (close to location **A** in Figure 1). In the age interval from 400 to 360 Ma, the Amuria block was situated in more southerly latitudes than the NCB. The paleolatitude difference between Siberia and NCB, and Siberia and Amuria is always significant during those times. The paleolatitude difference between Siberia (Late Devonian traps; 11.1°N, 149.7°E, A_{95} = 8.9°; [*Kravchinsky et al.*, 2002b]) and Amuria (Oldoy formation) in Late Devonian is $\Delta\lambda = 29.7° \pm 7.1°$, the rotation angle which likely took place later to close Mongol-Okhotsk ocean between Siberia and Amuria is $\Delta D = 179.8° \pm 12.0°$. Amuria was therefore close to, but independent of, NCB and significantly to the south of Siberia. This supports the idea that the Mongol-Okhotsk ocean between Siberia to the north and Amuria and north China to the south existed at least since 400 Ma ago (Figure 13). *Huang et al.* [2000] published a new result for Middle-Late Devonian (the pole is shown in Figure 12). The pole does not change the paleolatitude of the NCB but significantly changes its paleoposition. The corresponding rotation angle with the Oldoy pole, if this pole is used as a reference, is $\Delta D = 22.3°$

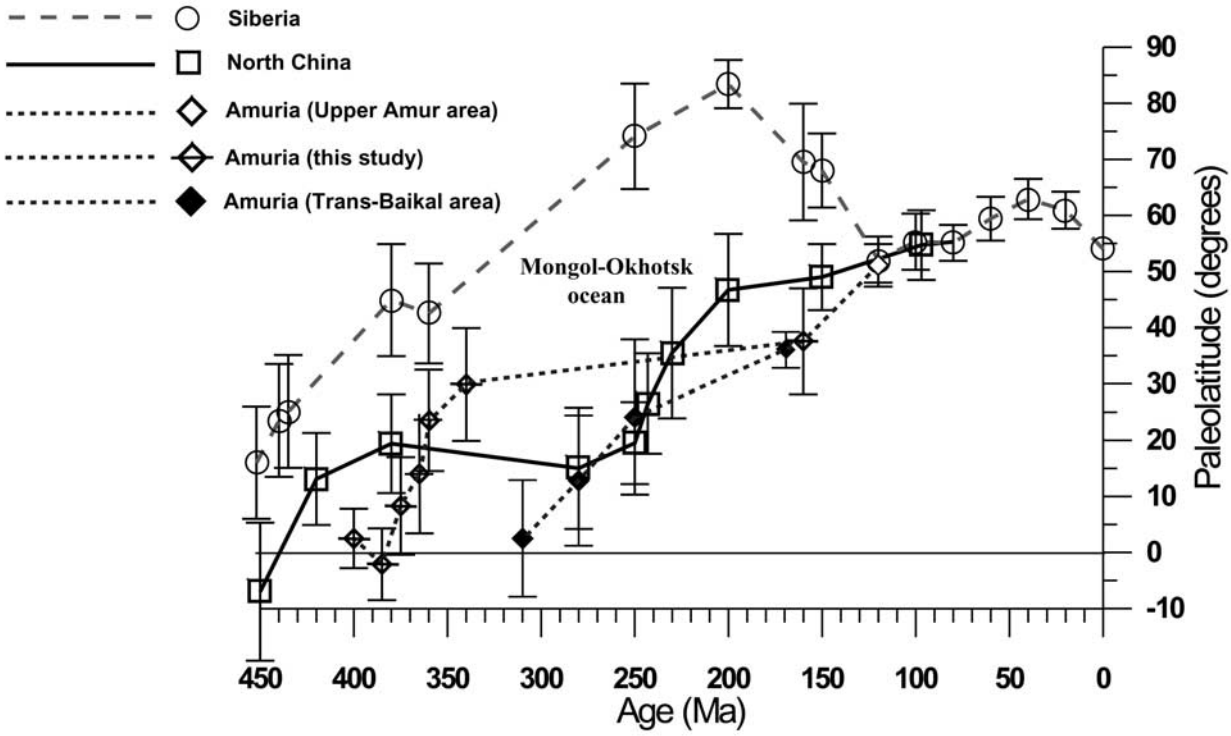

Figure 13. Paleolatitude plot for Upper Amuria region point situated on Mongol-Okhotsk suture (coordinates 54°N, 124°E). Open squares, expected paleolatitudes calculated from Eurasian APWP [*Bess and Courtillot*, 2002; *Van der Voo*, 1993] and Siberia [*Smethurst et al.*, 1998; *Kravchinsky et al.*, 2002b]; open circles, from north China APWP [*Enkin et al.*, 1992; *Zhao et al.*, 1996; *Gilder and Courtillot*, 1997]; diamonds, from Amuria block (this study). The paleolatitudes are plotted with dp coincidence cone 95% probability [*Fisher*, 1953].

± 9.2°, whereas the paleolatitude difference is $\Delta\lambda = -13.8° \pm 7.4°$. In this case, Amuria was very close to the NCB in terms of rotations during Middle-Late Devonian. There are no well defined Early Devonian poles for Siberia and the NCB, but on the basis of Silurian poles we could interpolate the relative positions of these blocks for this age. The late Carboniferous pole from Mongolia [*Pruner*, 1992] is rotated from the reference NCB pole (30°N, 11.9°E, A_{95} = 6.1° [*Zhao et al.*, 1996]) by $\Delta D = 39.4° \pm 12.2°$, and the paleolatitude difference is still significant at $\Delta\lambda = -19° \pm 9.6°$.

[37] On the basis of the late Permian poles from the Trans-Baikal region, we see that the paleolatitude difference between Amuria (Belektuy formation, Table 2) and Siberia (Permo-Triassic traps, [*Kravchinsky et al.*, 2002b]) is $\Delta\lambda = 48.5° \pm 7.5°$, and there is no longer any paleolatitudinal difference between Amuria and NCB (Middle Permian pole [*Zhao et al.*, 1996]) $-\Delta\lambda = 1.4° \pm 5.5°$. At the same time, we note that the Trans-Baikal region was apparently not a part of Upper Amuria (data from the Trans-Baikal area, together with Mongolian data after *Pruner* [1992], are marked as solid diamonds, whereas Upper Amur data from papers are marked as open diamonds). From Devonian to at least late Permian, Amuria may have consisted of number of minor blocks on the southern edge of the Mongol-Okhotsk ocean [*Zonenshain et al.*, 1990], which were possibly close to each other, but could have been separated in the Paleozoic (i.e., Central Mongolian, Argun, Upper Amur, Khingan-Bureya blocks). These blocks were subsequently accreted and thrust upon each other. We cannot follow in detail the differences between the Trans-Baikal and Upper Amur regions because poles from these regions are not synchronous. The Trans-Baikal area may have become accreted to the Upper Amur block before Middle-Late Jurassic. The relative rotation between the Trans-Baikalian Shadaron (Middle-Late Jurassic, pole 18, Table 2) and Upper Amurian Ayak (late Jurassic, pole 11, Table 2) formations is significant $\Delta D = 76° \pm 5.1°$, but there is no any paleolatitudinal difference ($\Delta\lambda = 2.3° \pm 3.3°$). The Early Cretaceous paleolatitude of Upper Amur area [*Halim et al.*, 1998a] is the same as for Siberia and north China (Figure 13). The ΔD differences of Amuria, both with respect to Siberia ($\Delta D = 78° \pm 6.7°$) and north China ($\Delta D = 72.3° \pm 10.7°$), might be easily explained in terms of postcollisional rotations during final stages of closing of the Mongol-Okhotsk ocean. There is no paleolatitude difference with either the NCB ($\Delta\lambda = 3.8° \pm 5°$), or Eurasia ($\Delta\lambda = 1.3° \pm 3.3°$). Upper Amuria was therefore probably rotated by some 75° counterclockwise with respect to Eurasia and China during post-Cretaceous collisional processes.

5.2. Paleopositions of the Amuria Block From the Devonian to the Present

[38] On the basis of our new paleomagnetic poles, we propose paleoreconstructions of the Amuria block relative to the Siberian platform [*Kravchinsky et al.*, 2002a, 2002b]

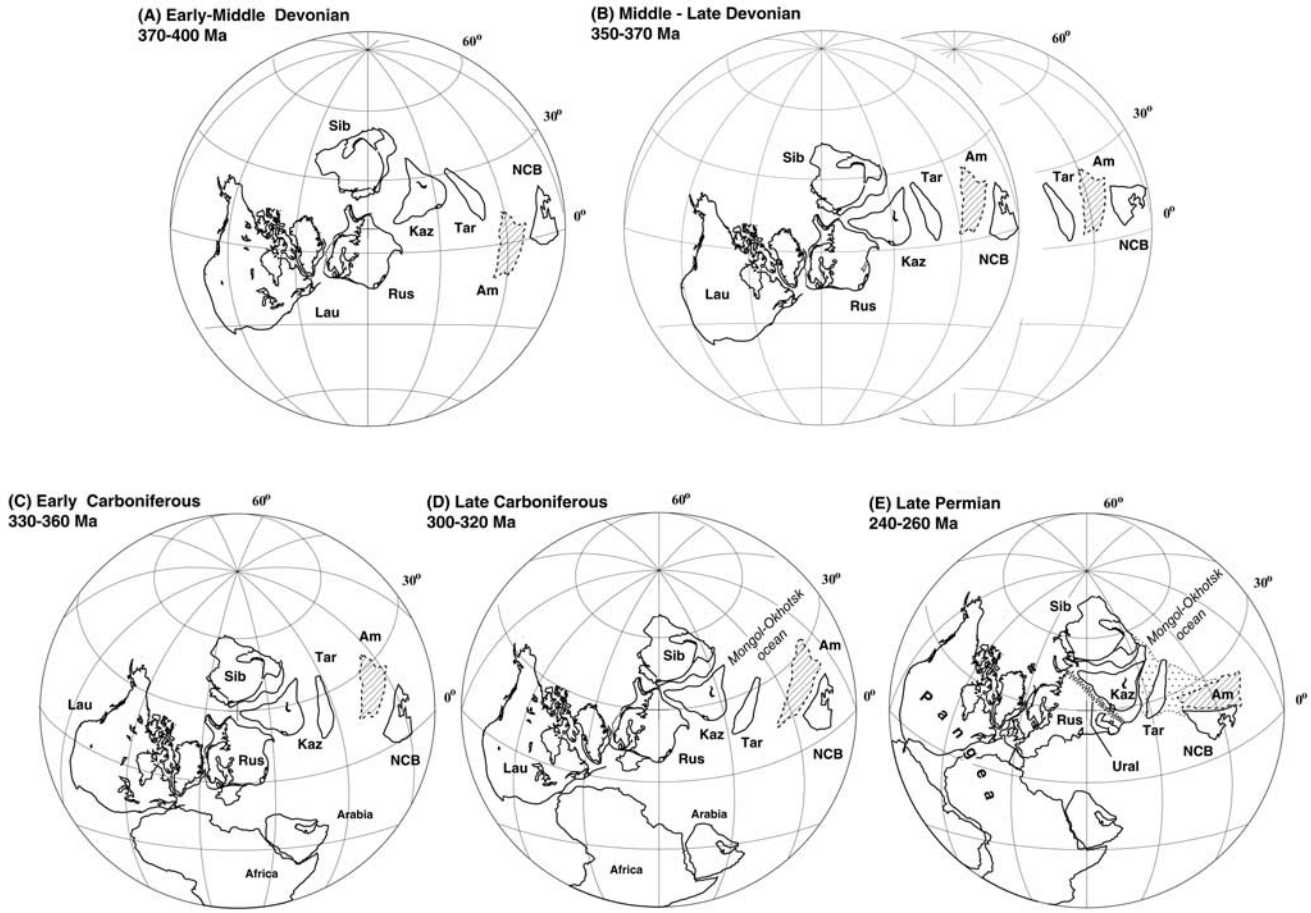

Figure 14. Schematic reconstructions of the Mongol-Okhotsk ocean from the Middle-Late Silurian to present time based on paleomagnetic data from Table 2. For Permian-Cretaceous we showed possible dry land (dotted area) between Eurasia and Chinese block to explain geological data, which suggest a Jurassic closure of the Mongol-Okhotsk ocean in the west Trans-Baikal region, our data evidence a still large paleolatitude difference between Amuria and Siberia blocks. For 350–370 Ma (Figure 14b) we showed two possibilities of North China Block paleoposition (left) after *Zhao et al.* [1996] and (right) after *Huang et al.* [2000] Names of blocks: Sib, Siberia; Amu, Amuria; Tar; Tarim; NCB, North China Block; Kaz, Kazakstan; Rus, Russian platform and Baltica; Lau; Laurentia.

and other related blocks from the Devonian to the Present (Figure 14). We used the Mongol-Okhotsk suture as the southern border of the Siberian platform. It is now generally accepted that the Mongol-Okhotsk ocean, lying between Siberia to the north (in present-day coordinates), and Amuria/north China to the south was closed between the Early Permian in eastern Mongolia and the Jurassic in Trans-Baikalia, and the Cretaceous in the Pacific part of Russia [*Kuzmin and Fillipova*, 1979; *Parfenov*, 1984; *Kravchinsky*, 1990; *Zonenshain et al.*, 1990; *Zhao et al.*, 1990; *Enkin et al.*, 1992; *Gusev and Khain*, 1995; *Xu et al.*, 1997; *Halim et al.*, 1998a; *Kravchinsky et al.*, 2002a]. Reconstruction of the North China platform relies on data by *Zhao et al.* [1996] and *Gilder and Courtillot* [1997]; paleopositions of the Amuria block for the Mesozoic and Cenozoic follow *Pruner* [1992], *Halim et al.* [1998a] and *Kravchinsky et al.* [2002a]; and paleopositions of the Tarim block follow *Bai et al.* [1987], *McFadden et al.* [1988], *Fang et al.* [1990], *Li et al.* [1990], and *Gilder et al.* [1996].

[39] In order to constrain the paleoposition of the Siberian platform, we used the APWP of Siberia from *Smethurst et al.* [1998] at 435 Ma, the poles of *Kravchinsky et al.* [2002b] at ~360 Ma and ~250 Ma and the APWP of Eurasia from 240 Ma to the Present [*Besse and Courtillot*, 1991; *Van der Voo*, 1993]. The new Paleozoic part of the APWP of Siberia is shown by a dashed line in Figure 12 on the basis of the 360 Ma pole from *Kravchinsky et al.* [2002b].

[40] Between 435 and 360 Ma, the Russian platform (with Baltica and a large part of western Europe) became part of Laurussia (Laurentia and Russia) [*Smethurst et al.*, 1998]. Unfortunately, there are no reliable paleomagnetic data for Siberia between 360 and 250 Ma. Northward motion of Siberia to high northern latitudes was associated with ~60° clockwise rotation between 360 (Figure 14) and 250 (Figure 14) Ma [*Kravchinsky et al.*, 2002b].

[41] *Zhao et al.* [1996] [see also *Van der Voo*, 1993; *Li et al.*, 1988] showed that north China was at the equator in the Middle Devonian (Figure 14). Based on the Middle-Late

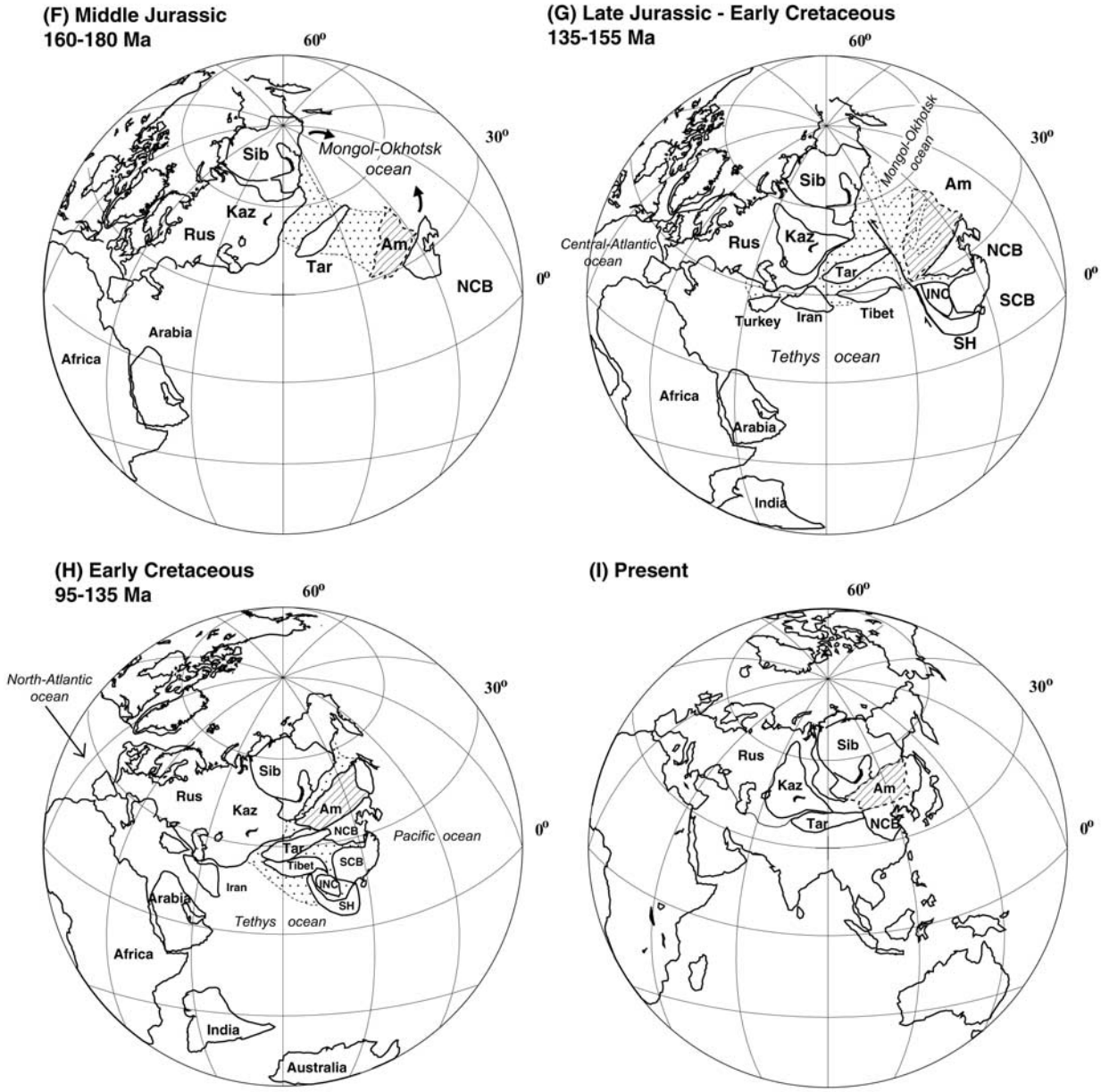

Figure 14. (continued)

Devonian pole for NCB of *Huang et al.* [2000], the NCB was at the same latitude as the Amuria microcontinent (Figure 14, left), but more rotated relative to Siberia ($\Delta D = 166.1° \pm 15.3°$). At this time Tarim was subequatorial, and moving northward [*Bai et al.*, 1987; *Fang et al.*, 1990; *Li et al.*, 1988]. The position of the Russian platform (with Baltica) is reconstructed after *Torsvik et al.* [1992, 1996]. Kazakhstan is positioned according to *Pechersky and Didenko* [1995]. The absolute dating of *Montero et al.* [2000] indicates that the closure of the Uralian paleo-ocean started in the south and migrated progressively northwards, between 320 (Figure 14) and 250 (Figure 14) Ma. During the Paleozoic, the Amurian blocks were always situated between north China and Siberia in equatorial to tropical latitudes, moving gradually to the North, from about 0° in Early-Middle Devonian to about 15° in Late Devonian, 20° in Early Carboniferous, and 30° in the late Permian (Figure 14).

[42] At 250 Ma, Siberia continued its clockwise rotation at high northern latitudes. The last stage of formation of northern Eurasia involved final accretion of Russia and Siberia along the Uralian belt. North Eurasia was incorporated into Pangea at this time [*Van der Voo*, 1993; *Torsvik et al.*, 1996; *Smethurst et al.*, 1998]. This could appear to somewhat contradict the estimates of *Zonenshain et al.* [1990] on the age of the collision between Amuria and Siberia. In effect, on the basis of the age of metamorphism and intraplate magmatism from the Mongolian Khingayn Mountains, these authors date the collision as Late Carboniferous–Early Permian for the western part of Amuria. This is related to the "scissors-like" closure of the Mongol-

Okhotsk ocean [*Zonenshain et al.*, 1990; *Zhao et al*, 1990], beginning at the end of the Carboniferous in the west. The data of *Kravchinsky et al.* [2002a] for the late Permian Belektuy (Amuria, Trans-Baikal area) and Alentuy (Siberia) formations (Table 2) suggest that a large oceanic gap remained between Amuria and Siberia in the Late Permian (at the longitude of the Belektuy sites): the paleolatitude difference between Alentuy and Belektuy localities amounts to 4750 ± 1850 km, whereas their present-day latitude difference is negligible [*Kravchinsky et al.*, 2002a].

[43] The very large rotations suggested by our new poles and the Early Cretaceous poles from *Halim et al.* [1998a] and *Kravchinsky et al.* [2002a] with respect to west Amuria (Trans-Baikal area and Mongolia) poles [*Pruner*, 1992] (Figure 12) may result from at least 3 complementary mechanisms, as proposed by *Kravchinsky et al.* [2002a]. (1) According to *Zonenshain et al.* [1990], the formation of the Amuria block resulted from the amalgamation of a number of microblocks (Khangay, Khentey, Central-Mongolian, Argun, Khingan-Bureya) in the Paleozoic. Part of the rotations could have arisen at the end of this history, from relative movements of these microblocks; (2) the post-Late Jurassic collision of Amuria and Siberia could probably produce significant local rotations, and (3) the suspected large left-lateral Tertiary shear related to incipient extrusion of Amuria due to indentation of India into Asia along the Mongol-Okhotsk suture as proposed by *Halim et al.* [1998b] provides a third possible mechanism for large rotations.

[44] South of the Mongol-Okhotsk ocean, the collision between the north China platform and the Amurian block was completed by the late Permian (Figure 14; compare the early Permian pole from Mongolia [*Pruner*, 1992] and the late Permian pole from the Trans-Baikal region - Belektuy pole, Table 2). There is no paleolatitude difference between the late Permian Belektuy formation and the NCB ($\Delta\lambda = 1.5^\circ \pm 5.5^\circ$).

[45] In the Triassic, the paleogeography remained close to that in the Late Permian, with clockwise rotation of Eurasia [*Besse and Courtillot*, 1991], and, as a result, continuing closure of the Mongol-Okhotsk ocean. Most of the Upper Amur sediments of Triassic-Jurassic age were remagnetized during the Cenozoic, probably linked to collisional processes [*Halim et al.*, 1998a].

[46] In the Jurassic, the latitude difference between the middle Jurassic Ayak (Upper Amur area) and late Jurassic Badin (Siberia) localities amounted to $\Delta\lambda = 35.5^\circ \pm 5.6^\circ$ (Table 2), whereas the present-day latitude difference is negligible. This difference cannot be directly expressed in terms of the width of the Mongol-Okhotsk ocean in Middle-Late Jurassic, because it also depends on the relative orientations of Siberia and Amuria at that time, but it shows that these localities remained far from each other in the Jurassic (Figure 14). This could reflect rapid north-south convergence of Amuria towards Siberia at the end of the Jurassic, as proposed by *Enkin et al.* [1992] and further supported by *Kravchinsky et al.* [2002a]. The new estimate is based on the middle Jurassic pole from the Upper Amur area and is about 1000 km less than the preliminary estimate of *Kravchinsky et al.* [2002a], which was based on a Middle-Late Jurassic pole from the Trans-Baikal region (pole 18, Table 2). A possible explanation of this difference in paleolatitudes between the Upper Amur and Trans-Baikal areas might be linked to their postearly Cretaceous final accretion, with shortening and overthrusting of the Unda-Daya block (where the Middle-Late Jurassic was studied) on to other regions of Trans-Baikalia [*Sizykh and Sapozhnikov*, 1971]. This interpretation matches the idea that the Mongol-Okhotsk ocean was closed by the beginning of the Cretaceous in the eastern part of suture (Figure 14), as suspected from the comparison of paleomagnetic data from NCB with the Eurasian APWP [e.g., *Besse and Courtillot*, 1991; *Enkin et al.*, 1992; *Yang et al.*, 1992] and data from early Cretaceous volcanic rocks of the Upper Amur region [*Halim et al.*, 1998a]. Late Triassic and Jurassic turbidites are described in the eastern part of the Mongol-Okhotsk suture. They include metabasites and cherts [*Turbin*, 1994; *Kozlovsky*, 1988] which possibly correspond to the last remnants of oceanic crust. At the same time we propose that the space which separated the Amuria block from Siberia (stippled area on Figure 14), was occupied by shallow sedimentary basins. The NE part was close to the Pacific ocean, whereas the SW part had a continental character: there are no marine sediments of Jurassic age in the western part of the Mongol-Okhotsk suture (Trans-Baikal area), whereas these are widespread all over the eastern part of the suture [*Zonenshain et al.*, 1990].

[47] Finally, we note that paleopoles from the southern margin of Siberia (north of the suture) are only slightly rotated with respect to the reference APWP poles, in contrast with the poles for formations south of the suture. The latter underline strong deformation within the Amuria block, after the Early Cretaceous, whereas the Siberian platform appears to have remained relatively unaffected. This is compatible with the hypothesis of *Halim et al.* [1998a] of eastward extrusion of the Amuria blocks.

[48] Our new data allow us to describe how the Mongol-Okhotsk embayment came to be formed as a result of relative motions of Siberia, Kazakhstan, Tarim, Amuria and north China from the early Devonian to the early Carboniferous. We are able to constrain the history of the Amurian block(s) during the subsequent evolution of this ''scissors-shaped'' ocean from the late Permian until its final closure no later than the early Jurassic [*Zonenshain et al.*, 1990; *Zhao et al*, 1990]. Two main phases of rotation of Amuria occur, a clockwise one in the early Permian and a counter-clockwise one in the early to middle Jurassic. Amuria remains at equatorial latitudes during the Devonian, then moves to ~20°N latitude by the late Carboniferous, and to ~45°N latitude by the end of the Jurassic, where it still lies. Paleomagnetic data show that the Amurian block(s) suffered significant internal deformation and rotations about vertical axes, whereas the southern margin of Siberia remained relatively undeformed as final closure with possible shear and slight extrusion determined the state of the Mongol-Okhotsk suture as we now see it.

[49] **Acknowledgments.** The authors express their deep gratitude for assistance in conducting the work and valuable advice to V. I. Golik, K. M. Konstantinov, L. P. Koukhar, M. A. Krainov, M. I. Kuzmin, V. A. Rybalko, and A. P. Sorokin. Special thanks for geological information and field trip help to K. D. Vakhtomin, without whose help this work would not have been possible. R. Enkin and J.-P. Cogné provided their free computer programs. We thank R. Enkin and F. Albarede for useful discussion and their suggestions, which improved this paper. This research was funded by

the Amur region Geological Survey and Institut de Physique du Globe de Paris. V. A. Kravchinsky is also thankful to J.-P. Valet, J.-P. Cogné, and J. Besse for their useful discussion and help during his stay in France; to Ted Evans for his support at the University of Alberta; and to A. Kamal for her kind help in settling in Canada. This is contribution 1845 of Institut de Physique du Globe de Paris.

References

Bai, Y., G. Chen, Q. Sun, Y. Sun, Y. Li, Y. Dong, and D. Sun, Late Paleozoic polar wander path for the Tarim platform and its tectonic significance, *Tectonophysics*, *139*, 145–153, 1987.

Besse, J., and V. Courtillot, Revised and synthetic apparent polar wander paths of the African Eurasian, North American and Indian plates, and true polar wander since 200 MA, *J. Geophys. Res.*, *96*, 4029–4050, 1991.

Besse, J., and V. Courtillot, Apparent and true polar wander and the geometry of the geomagnetic field for the last 200 Myr, *J. Geophys. Res.*, 10.1029/2000JB000050, in press, 2002.

Enkin, R. J., Formation et deformation de l'Asie depuis la fin de l'ere primaire: Les apports de l'etude paleomagnetique des formations secondaires de Chine du Sud, Ph.D. thesis, 333 pp., Univ. de Paris 7, Paris, 1990.

Enkin, R. J., Z. Yang, Y. Chen, and V. Courtillot, Paleomagnetic constraints on the geodynamic history of the major blocks of China from the Permian to the Present, *J. Geophys. Res.*, *97*, 13,953–13,989, 1992.

Fang, D., H. Chen, G. Jin, Y. Guo, Z. Wang, X. Tan, and S. Yin, Late Paleozoic and Mesozoic paleomagnetism and tectonic evolution of the Tarim terrane, in *Terrane Analysis of China and the Pacific Rim, Earth Sci. Ser.*, vol. 13, edited by T. J. Wiley, D. G. Howell, and F. L. Wong, pp. 251–255, Circum-Pac. Counc. for Energy and Miner, Resour., Houston, Tex., 1990.

Fisher, R., Dispersion on a sphere, *Proc. R. Soc. London, Ser. A*, *217*, 295–305, 1953.

Freidin, A. I., State geological map of the USSR (in Russian), Amur-Zeya area, 80 pp., scale 1:200,000, sheet N-51-XXII, Nedra, Moscow, 1966.

Gilder, S., and V. Courtillot, Timing of the north-south China collision from new middle to late Mesozoic paleomagnetic data from the North China Block, *J. Geophys. Res.*, *102*, 17,713–17,727, 1997.

Gilder, S., X. Zhao, R. Coe, Z. Meng, V. Courtillot, and J. Besse, Paleomagnetism and tectonics of the southern Tarim basin, northwestern China, *J. Geophys. Res.*, *101*, 22,015–22,031, 1996.

Gusev, G. S., and V. E. Khain, About relationship of Baikal-Patom, Aldan-Vitim and Mongol-Okhotsk terrains (south of Middle Siberia), *Geotektonika*, *5*, 68–82, 1995.

Halim, N., V. Kravchinsky, S. Gilder, J.-P. Cogné, M. Alexutin, A. Sorokin, V. Courtillot, and Y. Chen, A palaeomagnetic study from the Mongol-Okhotsk region: Rotated Early Cretaceous volcanics and remagnetized Mesozoic sediments, *Earth Planet. Sci. Lett.*, *159*, 133–145, 1998a.

Halim, N., J.-P. Cogné, Y. Chen, R. Atasiei, J. Besse, V. Courtillot, S. Gilder, J. Marcoux, and R. L. Zhao, New Cretaceous and Early Tertiary paleomagnetic results from Xining-Lanzhou basin, Kunlun and Qiangtang blocks, China: Implications on the geodynamic evolution of Asia, *J. Geophys. Res.*, *103*, 21,025–21,045, 1998b.

Halls, H. C., A least-squares method to find a remanence direction from converging remagnetization circles, *Geophys. J. R. Astron. Soc.*, *45*, 297–304, 1976.

Huang, B. C., Y. Otofuji, Z. Y. Yang, and R. Zhu, New Silurian and Devonian palaeomagnetic results from the Hexi Corridor terrane, northwest China and their tectonic implications, *Geophys. J. Int.*, *140*, 132–146, 2000.

Jelinek, V., A high sensitive spinner magnetometer, *Stud. Geophys. Geod.*, *10*, 58–78, 1966.

Jelinek, V., Precision A.C. bridge set for measuring magnetic susceptibility and its anisotropy, *Stud. Geophys. Geod.*, *17*, 36–48, 1973.

Kirschvink, J. L., The least-squares line and plane and the analysis of paleomagnetic data, *Geophys. J. R. Astron. Soc.*, *62*, 699–718, 1980.

Kozak, Z. P., K. D. Vakhtomin, A. S. Davidov, and M. N. Shilova, State geological map of the Russian Federation (in Russian), scale 1:200,000, Stanovoy area, 2nd issue, sheet N-51-XVI, 196 pp., Nedra, St. Petersburg, 2001.

Kozak, Z. P., A. S. Davidov, S. N. Belikov, M. N. Shilova, A. E. Chugaev, and L. V. Shishkin, State geological map of the Russian Federation (in Russian), scale 1:200,000, Zeya area, 2nd issue, sheet N-51-XXI, 196 pp., Nedra, St. Petersburg, 2002.

Kozlovsky, E. A., (Ed.), *Geology of the BAM Zone*, vol. 1, *Geological Structure* (in Russian), 420 pp., Nedra, St. Petersburg, 1988.

Kravchinsky, V. A., Paleomagnetism of rocks of Mongol-Okhotsk geosuture, *Publ. IGCP Proj. 224 and 283*, pp. 146–149, Inst. of Geol. and Geophys., Siberian Branch of the Russ. Acad. of Sci., Novosibirsk, Russia, 1990a.

Kravchinsky, V. A., Horizontal movements of tectonic blocks of the Mongol-Okhotsk geosuture (in Russian), in *Present Geophysical Investigations of Eastern Siberia*, pp. 102–105, Irkutsk Publ., East. Siberian Pravda, Russia, 1990b.

Kravchinsky, V. A., Paleomagnetic study in Mongol-Okhotsk folded belt (in Russian), Ph.D. thesis, 181 pp., Irkutsk State Tech. Univ., Irkutsk, 1995.

Kravchinsky, V. A., J.-P. Cogné, W. Harbert, and M. I. Kuzmin, Evolution of the Mongol-Okhotsk ocean with paleomagnetic data from the suture zone, *Geophys. J. Int.*, *148*, 34–57, 2002a.

Kravchinsky, V. A., K. M. Konstantinov, V. Courtillot, J.-P. Valet, J. I. Savrasov, S. D. Cherniy, S. G. Mishenin, and B. S. Parasotka, Paleomagnetism of east Siberian traps and kimberlites: Two new poles and paleogeographic reconstructions at about 360 and 250 Ma, *Geophys*., *J. Int.*, *148*, 1–33, 2002b.

Kuzmin, M. I., and I. B. Fillipova, The history of the Mongol-Okhotsk belt in the Middle–Late Paleozoic and Mesozoic, in *Lithospheric Plate Structure* (in Russian), edited by L. P. Zonenshain, pp. 189–226, Inst. of Oceanol., Russ. Acad. of Sci., Moscow, 1979.

Li, Y. P., Z. K. Zhang, M. McWilliams, R. Sharps, Y. J. Zhai, Y. A. Li, Q. Li, and A. Cox, Mesozoic paleomagnetic results of the Tarim craton: Tertiary relative motion between China and Siberia, *Geophys. Res. Lett.*, *15*, 217–220, 1988.

Li, Y., M. McWilliams, R. Sharps, A. Cox, Y. Li, Q. Li, Z. Gao, Z. Zhang, and Y. A. Zhai, Devonian paleomagnetic pole from red beds of the Tarim Block, China, *J. Geophys. Res.*, *95*, 19,185–19,198, 1990.

Li, Z. X., C. M. Powell, and A. Trench, Palaeozoic global reconstructions, in *Palaeozoic Vertevrate Biostratigraphy and Biogeography*, edited by J. A. Long, pp. 25–53, Belhaven, London, 1993.

Mamontov, Y. A., State geological map of the USSR (in Russian), Amur-Zeya area, explanation, 92 pp., scale 1:200,000, sheet N-51-XX, Nedra, Moscow, 1972.

McElhinny, M. W., Statistical significance of the fold test in paleomagnetism, *Geophys. J. R. Astron. Soc.*, *8*, 338–340, 1964.

McFadden, P. L., and F. J. Lowes, The discrimination of mean directions drawn from Fisher distributions, *Geophys. J. R. Astron. Soc.*, *67*, 19–33, 1981.

McFadden, P. L., and M. W. McElhinny, The combined analysis of remagnetization and direct observation in paleomagnetism, *Earth Planet. Sci. Lett.*, *87*, 161–172, 1988.

McFadden, P. L., and M. W. McElhinny, Classification of the reversal test in paleomagnetism, *Geophys. J. Int.*, *103*, 725–729, 1990.

McFadden, P. L., X. H. Ma, M. W. McElhinny, and Z. K. Zhang, Permo-Triassic magnetostratigraphy in China: Northern Tarim, *Earth Planet. Sci. Lett.*, *87*, 152–160, 1988.

Montero, P., F. Bea, A. Gerdes, G. Fershtater, E. Zin'kova, N. Borodina, T. Osipova, and V. Smirnov, Single-zircon evaporation ages and Rb–Sr dating of four major Variscan batholiths of the Urals: A perspective on the timing of deformation and granite generation, *Tectonophysics*, *317*, 93–108, 2000.

Natal'in, B. A., and C. B. Borukaev, Mesozoic sutures of the south of the Russian far east (in Russian), *Geotectonics*, *1*, 84–97, 1991.

Ol'kin, G. F., A. G. Stark, and Y. I. Starikov, State geological map of the USSR (in Russian), Amur-Zeya area, 90 pp., scale 1:200,000, sheet N-51-XXI, Nedra, Moscow, 1971.

Parfenov, L. M., *Continental Margins and Island Arcs of Mesozoids of North-Western Asia* (in Russian), 192 pp., Nauka, Moscow, 1984.

Parfenov, L. M., L. I. Popeko, and O. Tomurtogoo, The problems of the tectonics of the Mongol-Okhotsk orogene (in Russian), *Geol. Pac. Ocean*, *18*(5), 24–43, 1999.

Pavlenko, M. V., State geological map of the USSR (in Russian), 80 pp., scale 1:200,000, sheet N-51-XIX, Nedra, Moscow, 1966.

Pechersky, D. M., and A. N. Didenko, *Paleozoic Ocean, Petromagnetic and Paleomagnetic Information of the Lithosphere* (in Russian), OEFZ RAN, Moscow, 1995.

Pisarevsky, S. A., Paleomagnetic directions and pole positions: Data for the USSR, Issue 5, Sov. Geophys. Comm., World Data Cent.-B, Moscow, 1982.

Pospelova, G. A., Paleomagnetic directions and pole positions: Data for the USSR, Issue 1, Sov. Geophys. Comm., World Data Cent.-B, Moscow, 1971.

Pruner, P., Paleomagnetism and paleogeography of Mongolia in the Cretaceous, Permian and Carboniferous: Final report, *Phys. Earth Planet. Inter.*, *70*, 169–177, 1992.

Sengor, A. M. C., and B. A. Natal'in, Paleotectonics of Asia: Fragments of a synthesis, in *The Tectonic Evolution of Asia*, edited by A. Yin and M. Harrison, pp. 486–640, Cambridge Univ. Press, New York, 1996.

Sizykh, V. I., and V. P. Sapozhnikov, Geological map of the USSR (in Russian), West Trans-Baikal series, 90 pp., scale 1:200,000, sheet M-49-VII, Nedra, Moscow, 1971.

Smethurst, M. A., A. N. Khramov, and T. H. Torsvik, The Neoproterozoic and Palaeozoic palaeomagnetic data for the Siberian Platform: From Rodinia to Pangea, *Earth Sci. Rev.*, *43*, 1–21, 1998.

Sorokin, A. A., Geochemistry and geodynamic position of magmatic rocks of the central segment of the Mongol-Okhotsk fold belt (in Russian), Ph.D. thesis, 156 pp., Inst. of Geochem., Siberian Branch of the Russ. Acad. of Sci., Irkutsk, Russia, 1992.

Sorokin, A. A., S. I. Dril, and M. I. Kuzmin, Rock geochemistry and paleodynamic setting of the Jankan ophiolite (Mongol-Okhotsk fold belt) (in Russian), in *Geodynamics and Evolution of the Earth, Proceedings of the Conference RFBR*, edited by N. L. Dobretsov, pp. 69–70, Siberian Branch of the Russ. Acad. of Sci., Irkutsk, Russia, 1996.

Torsvik, T. H., M. A. Smethurst, R. Van der Voo, A. Trench, N. Abrahamsen, and E. Halvorsen, Baltica: A synopsis of Vendian-Permian palaeomagnetic data and their palaeotectonic implications, *33*, 133–152, 1992.

Torsvik, T. H., M. A. Smethurst, J. G. Meert, R. Van der Voo, W. S. McKerrow, M. D. Brasier, B. A. Sturt, and H. J. Walderhaug, Continental break-up and collision in the Neoproterozoic and Palaeozoic: A tale of Baltica and Laurentia, *Earth Sci. Rev.*, *40*, 229–258, 1996.

Turbin, M. T., (Ed.), Decisions of IV Inter-Organizational Regional Stratigraphic Meeting for Precambrian and Phanerozoic Epoch at south of far east and eastern Trans-Baikalia, (in Russian), 124 pp., Khabarovsk State Mine-Geol. Co. House, Khabarovsk, Russia, 1994.

Van der Voo, R., *Paleomagnetism of the Atlantic, Tethys, and Iapetus Oceans*, 411 pp., Cambridge Univ. Press, New York, 1993.

Vinarsky, Y. S., A. N. Zhitkov, and A. Y. Kravchinsky, Automated system OPAL for processing paleomagnetic data, algorithms and programmes (in Russian), 86 pp., *Issue 0/99/VIAMS*, VIAMS (All-Soviet Union Institute of Automatic and Mechanic Systems), Moscow, 1987.

Watson, G. S., and R. J. Enkin, The fold test in paleomagnetism as a parameter estimation problem, *Geophys. Res. Lett.*, *20*, 2135–2137, 1993.

Xu, X., W. Harbert, S. Drill, and V. Kravchinsky, New paleomagnetic data from the Mongol-Okhotsk collision zone, Chita region, south-central Russia: Implications for Paleozoic paleogeography of the Mongol-Okhotsk Ocean, *Tectonophysics*, *269*, 113–129, 1997.

Yang, Z., V. Courtillot, J. Besse, X. Ma, L. Xing, S. Xu, and J. Zhang, Jurassic paleomagnetic constrains on the collision of the North and South China blocks, *Geophys. Res. Lett.*, *6*, 577–580, 1992.

Zhao, X., R. S. Coe, Y. X. Zhou, H. R. Wu, and J. Wang, New palaeomagnetic results from northern China: Collision and suturing with Siberia and Kazakhstan, *Tectonophysics*, *181*, 43–81, 1990.

Zhao, X., R. S. Coe, S. A. Gilder, and G. M. Frost, Paleomagnetic constraints on the palaeogeography of China: Implications for Gondwanaland, *Aust. J. Earth*, 643–672, 1996.

Zijderveld, J. D. A., A.C. demagnetization of rocks, analysis of results, in *Methods in Paleomagnetism*, edited by D. W. Collinson, K. M. Creer, and S. K. Runcorn, pp. 254–286, Elsevier Sci., New York, 1967.

Zonenshain, L. P., M. I. Kuzmin, and L. M. Natapov, *Tectonics of Lithosphere Plates of the Territory of the USSR* (in Russian), vol. 1, 328 pp., Nedra, Moscow, 1990.

V. Courtillot, Laboratoire de Paléomagnétisme, Institut de Physique du Globe de Paris, 4 place Jussieu, 75252 Paris Cedex 05, France. (courtil@ipgp.jussieu.fr)

V. A. Kravchinsky, Physics Department, University of Alberta, Edmonton, AB, T6G 2J1, Canada. (vkrav@phys.ualberta.ca)

A. A. Sorokin, Division of the Regional Geology and Hydrogeology, Far East Branch of Russian Academy of Science, B. Khmelnitsky st., 2, Blagoveshchensk, 675000, Russia. (sorokin@asc.blg.ru)

View publication stats